Renewable and Sustainable Energy Reviews 87 (2018) 77–95

Contents lists available at ScienceDirect

Renewable and Sustainable Energy Reviews

journal homepage: www.elsevier.com/locate/rser

Optimal selection of air expansion machine in Compressed Air Energy Storage: A review

Wei He[a], Jihong Wang[a,b,*]

[a] School of Engineering, University of Warwick, Coventry CV4 7AL, United Kingdom
[b] School of Electrical & Electronic Engineering, Huazhong University of Science & Technology, China

ARTICLE INFO

Keywords:
Compressed Air Energy Storage
Expander Classification
Expander Modelling
Optimal Expander Selection

ABSTRACT

Electrical energy storage has been recognised as an underpinning technology to meet the challenges in the power network arisen from the rapidly increasing penetration of renewable energy. Compressed Air Energy Storage (CAES) has gained substantial worldwide attention in recent years due to its low-cost and high-reliability in the large-scale energy storage systems. Air expander is one of the key components in a CAES system because its operational characteristics determine the power conversion efficiency and the power generation during the discharge period. The performance of the expander contributes heavily to the round trip efficiency of the whole system. This paper presents an up-to-date review of the CAES technology, and methods for modelling and selecting expanders for CAES systems. The focuses of selecting the appropriate expansion machines are identifying and analysing the characteristics of both CAES systems and expansion machines, and finding the matched expanders for the CAES system formulation (i.e. diabatic, adiabatic and isothermal CAES) and operational conditions (i.e. air pressure, temperature and flow rate). After all, recommendations and guidelines in selecting appropriate expanders and expansion stage numbers are formulated and discussed; this laid a step stone for choosing suitable expansion machines to achieve an overall CAES system high efficiency.

1. Introduction

Carbon dioxide emission, one of the major causes for global warming, has been recognised as a pressing issue and needs to be tackled in this generation [1]. To address this issue, reducing use of fossil fuels is unavoidable, which calls for power generation from renewable energy sources to meet the electricity demand. It has been evidenced by the rapidly increased penetration of renewable energy to the power network in recent years [2–5]. In 2014, power from renewable energies represented approximately 58.5% of the net additions to the global power generation capacity, with considerable growths in all regions [6]. By the end of 2014, renewables, mainly wind, solar PV and hydro power, accounted for an estimated 27.7% of the world's power generation capacity, enough to supply 22.8% of global electricity [6]. However, due to the inherent intermittence of the most renewable energy sources, there is a great challenge in the power generation and load balance to maintain the stability and reliability of the power network [7]. While various solutions are sought, energy storage has been recognised as one of the feasible technologies to address these issues, which facilitates the power balancing by decoupling the generation and consumption in the time and space domains through multiple charging and discharging cycles [8].

Based on the form of energy stored in the system, major energy storage technologies include mechanical (pumped hydro, compressed air, and flywheel), electrochemical (batteries), electrical (capacitors), chemical (hydrogen with fuel cells), and thermal energy storage. Technical characteristics of the selected energy storage technologies are listed in Table 1. Mechanical storage systems, has long lifetime, low energy capital cost, and much larger power/energy rating than other energy storage technologies listed in Table 1. Therefore, they are suitable for time shifting, load shaving, load levelling, and seasonal energy storage. As one of the two large-scale commercialised energy storage technologies, large-scale commercialised Compressed Air Energy Storage (CAES) plants which are able to provide rated power capacity over 100 MW by single generation unit, have demonstrate to be reliable in the large-scale energy management [9].

Because the maturity of Pumped Hydro Energy Storage (PHES), the PHES plants have been deployed worldwide. However, these commercialised large-scale plant are subject to severe geographic restrictions. A site for a PHS plant must be suitable for the construction of standing or dammed-up water reservoirs with very large volumes for storing water [10]. In fact, the number of installation of new PHES plants has inclined

* Corresponding author at: School of Engineering, University of Warwick, Coventry CV4 7AL, United Kingdom.
E-mail address: Jihong.wang@warwick.ac.uk (J. Wang).

https://doi.org/10.1016/j.rser.2018.01.013
Received 22 July 2016; Received in revised form 10 October 2017; Accepted 30 January 2018
Available online 23 February 2018

Table 1
Characteristics of several energy storage technologies. These characteristics listed in the table are summarised from the review and comparisons in [23].

Characteristics	Large-scale CAES	Small CAES	PHES	Li-ion battery	Lead acid battery	Super-capacity	Hydrogen fuel
Power density, W/L	0.5–2	> large-scale CAES	0.5–1.5	1500–10,000	10–400	> 100,000	> 500
Energy density, Wh/L	2–6	> large-scale CAES	0.5–2	200–500	50–90	10–30	500–3000
Rated power rating, MW	100–1000	0.003–3 potential to 10	100–5000	0–100	0–40	0–0.3 +	< 50
Rated energy capacity, MWh	< 1000	< ~ 0.01	500–8000	0–10	0–40	0–0.0005	0.312 and 39
Lifetime, year	20–40	> 23	40–60	5–16	5–15	10–30	5–20
Cycle efficiency	40–70%	–	70–85%	75–97%	63–90%	84–95%	20–66%
Response time	Minutes	Seconds-minutes	Minutes	Milli-seconds	Milli-seconds	Milli-seconds	Seconds
Power capital cost, $/kWh	400–1000	517–1550	2000–4000	900–4000	300–600	100–450	500–3000
Energy capital cost, $/kWh	2–120	200–250	5–100	600–3800	200–400	300–2000	2–15

since 90's due to the environmental concerns and the scarcity of favourable sites [11]. The potential for the further major PHES schemes would also be restricted [12]. Different from the PHES plant, in a CAES system, air, instead of water, is compressed and released by compressors and expanders to fulfil a cycle of charge and discharge [13]. Although the large-scale storage of the compressed air is also restricted by geologic conditions, there are much more available sites for a large-scale CAES plant than the available sites for PHES. Porous rock reservoirs (aquifers or existing depleted gas reservoirs) and cavern reservoirs (caverns in salt formation and low-permeability hard rock) are appropriate for CAES. For example, existing gas storage facilities for natural gas storage might be suitable for storing compressed air [14].

Excluding the successful applications in the large-scale energy storage, with the continuous development of CAES, small-scale systems of CAES are also explored in both academic studies and industrial projects [15–18]. Prototypes of micro-scale and small-scale CAES systems emerged as the alternatives to the electrical or electrochemistry based energy storage technologies, such as batteries [19] and super-capacitors [20]. To compete with the well-developed high energy/power density electrical and electrochemical energy storage technologies as listed in Table 1, small scale CAES systems have several advantages, such as low self-discharge, long life-time, low-maintenance, reliable even in hostile environments, etc. Although there are several published reviews of energy storage systems in which potential benefits of CAES have been recognised [21–24], and a recent overview on CAES history and system classification [25], limited studies were reported on the optimal selection of the CAES system components. Most recently, Marvania and Subudhi presented a comprehensive review of compressed air power engines for vehicles in which the propulsion system is quite similar to CAES [26]. Nevertheless, the power capacity and energy density of the compressed air power engines are limited and significantly smaller than those used in many CAES systems.

In a CAES system, the expander is a critical component in determining the rated power output and the overall energy conversion efficiency. The selection of expanders in formulating a CAES system highly depends on both the system operations and the discharge power capacity of the energy storage system [27]. Generally, two main types of expanders can be distinguished from the market: the positive displacement (volume) type, such as reciprocating expander, screw and scroll expanders, and the dynamic (velocity) types, such as radial and axial turbines. To select an appropriate expansion machine, several reviews of applications and guidelines of different expansion machines have been reported in the studies of organic Rankine cycle (ORC). Qiu et al. reviewed various expansion machines and discussed the principles of selecting different types of expanders for ORC-based micro-CHP (combined heat and power) systems [28]. Bao and Zhao discussed all types of expansion machines' operating characteristics, aimed to guide the selection of expanders for an efficient ORC system [29]. Lemort et al. compared different expansion machines, especially for the positive displacement types including reciprocating, screw and scroll expanders, in ORC systems with different working fluids [30–34].

Compared to heat engines such as ORC, CAES has its unique characterisations: 1) air is the working fluid to fulfil the charge and discharge processes; 2) compared to heat engines which generate electricity between two heat sources, the potential of air, i.e. air pressure, plays a much significant role in CAES; and 3) CAES systems charge and discharge associating with multiple heat sources in a variety of ways. Therefore, although the experiences from the design of expanders in traditional heat engine cycles are beneficial, specific considerations and requirements for expander's design are needed for different CAES system types. However, from the published literatures, there is lack of guidelines on selection of expansion machines to fit and match the CAES system formulations. To fill the knowledge gap and enable optimal selection and design of expanders in CAES, tools for simulations of a CAES system considering the expanders' geometric parameters are essential. Rather than general thermodynamic analysis, requirements for a expander model used in CAES system modelling are not only accurate sufficiently to present the characteristics of the expander at the component-level, but also efficient in computation and compatible to be integrated to a system-level simulation.

Therefore, this study aims to compare different expansion machines and their potential applications in CAES systems, and review the associated mathematical models which are suitable for a system-level modelling. In order to provide a state-of-the-art picture of CAES technology development and a guideline of selecting appropriate expansion machines in practice, this review covers: 1) an overview of CAES system types, and 2) a comparative discussion of expansion machine types and their applications in CAES systems. For deriving the principles for recommendations of expanders, classifications of the current CAES systems are introduced. According to the energy flow in a CAES system, three major types of CAES are discussed to form the fundamental principles in choosing appropriate expanders. Then, several machine types of expanders are briefly introduced, including both volumetric and dynamic types. Finally, recommendations of expanders subject to CAES system types and scales are made and a generic preliminary system/component design procedure is also discussed.

2. Overview and comparison of CAES system formulation

In general, a CAES system refers to a process of converting electrical energy to a form of compressed air for energy storage and then it is converted back to electricity when needed. An illustrated conventional CAES system is plotted in Fig. 1. During the charge process, air is pressurised by compressors which are driven by motors using off-peak electricity from the grid or/and renewable energy. Before the storage and the compression, the compressed air flows through interconnected heat exchangers or other heat sinks to decrease its temperature. During the discharge period, the compressed air is first heated by the heat exchangers or other heat sources and produce work by expanders. The mechanical work is converted to electricity by connecting electric generators to the expander's shaft. Five major sub-processes formulate a complete CAES system: 1) air compression; 2) heat exchanges during both charge and discharge; 3) air expansion; 4) compressed air storage in cavity or pressure container/tank; and 5) mechanical transmission

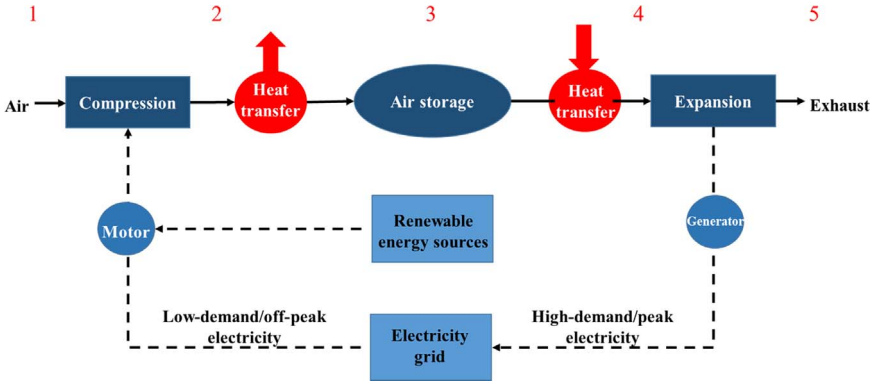

Fig. 1. Schematic diagram of a conventional CAES.

between motor, generator, compressor, and expander.

Depending on the scale of a CAES system, it can be roughly divided into large-scale CAES (> 100 MW), micro-scale CAES (tens of kW) and small-scale CAES ranged in between. Large-scale CAES systems are normally built for grid applications in load shifting, peak shaving, and frequency/voltage control [21]. Small-scale CAESs are more suitable for integration with renewable energy for back-up, load following and uninterruptible power supply. An application of small-scale CAES system for load following was presented in [35] in which an approach of investigating and controlling was also used to minimise the specific compression work. Micro-scale CAES is capable to be used in a multi-purpose system. A good example of a micro-scale CAES combines energy storage, air cycle heating and cooling was analysed in [36]. Proper types of expansion machines suit different CAES system scales and operations. High performance of these systems is only achieved when appropriate compressors and expanders are selected. As a matter of fact, overall performance of a CAES system is significantly affected by the efficiencies of air compression and expansion processes, because they are the "interfaces" to transfer different energies where significant exergy loss normally occurs. In a cycle from the charge to the discharge, more stages of the compression and expansion processes are used, more sensitive are the compressor's and expander's efficiencies to the overall round trip efficiency. It was demonstrated that the isentropic efficiencies of compressors and expanders/turbines are the two most influential parameters impacting the overall CAES performance [37].

Depending on trajectories of air compression and expansion from state 1–5 as shown in Fig. 1, CAES can be mainly divided into three categories: conventional diabatic CAES (D-CAES), adiabatic CAES (A-CAES), and isothermal CAES (I-CAES). An illustration of these three CAES systems are shown in Fig. 2 in which States 1–5 present initial air, compressed air, stored air, discharged air and exhaust air as illustrated in Fig. 1. D-CAES, A-CAES and I-CAES are illustrated in Fig. 2(a)–(c), respectively.

2.1. Diabatic compressed air energy storage

Conventional D-CAES can be considered as a CAES assisted gas turbine cycle. Therefore, similar to conventional thermal power plant applying Brayton cycle, the performance of the plant is determined by its thermal efficiency. The intrinsic nature of heat engines indicates that an increase in the temperature differences between the heat sources directly enhances the thermal efficiency of the cycle. However, in a D-CAES, excluding heat generated by combustion as a portion of energy input, off-peak electricity, another part of energy input, is also converted into the energy potential of compressed air which is stored in the cavern and released at the peak-period. As shown in Fig. 2(a), because of the heat produced by combustion (Q_{in}), temperature of the air from the state 3 which is the compressed air stored is significantly increased to the state 4. Consequently, more work can be generated in the expansion process from the state 4 to the state 5 compared to the stand-alone Brayton cycle.

Until now there are two CAES plants in operation in the world. The first utility-scale CAES project is the 290 MW (upgraded to 321 MW) Huntorf plant in Germany using salt dome, which was built in 1978. The other is a 110 MW plant with a capacity of 26 h in McIntosh, Alabama. These traditional D-CAES systems have been demonstrated to be successfully operated in realistic for several decades. The Huntorf CAES plant has reliably operated with excellent performance with 90% availability and 99% starting reliability for the last 30 years and still in good condition [38]. McIntosh CAES plant also has maintained an average starting reliability of between 91.2% and 92.1%, and an average running reliability of 96.8% and 99.5% for discharge and charge periods respectively [38]. At present, several CAES plants are being constructed or projected to be constructing worldwide. For example, a 300 MW CAES installation using a saline porous rock formation being developed near Bakersfield in California and another 150 MW salt-based CAES is also being developed in Watkins Glen, New York [39]. However, D-CAES has some disadvantages such as considerate thermal losses, dependence of fossil fuel and requirement of

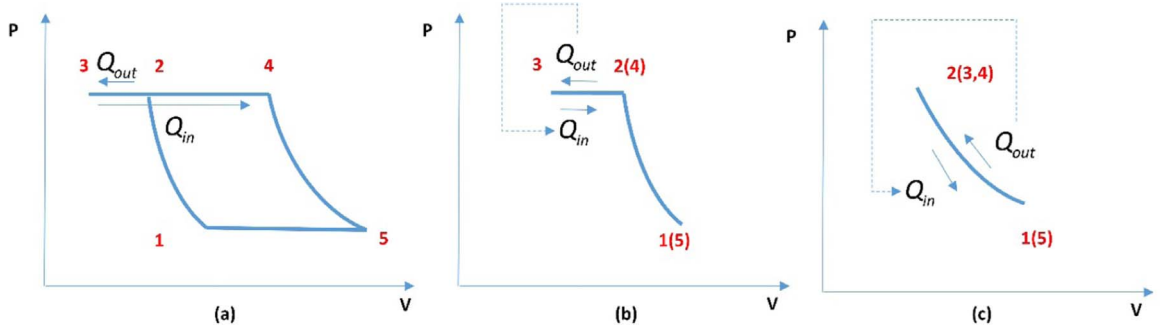

Fig. 2. P-V diagram of different CAES systems in which illustrated P-V diagrams of D-CAES, A-CAES and I-CAES are shown in (a)–(c), respectively.

geological formations.

To overcome these disadvantages, some improvements have been made to increase the performance of D-CAES. In McIntosh CAES plant, thermal energy of the exhausted gas is recovered using Recuperator to increase the temperature of the compressed air before flowing to the high-pressure turbine. Accordingly, it reduces one-quarter of fuel consumption and leads to the round trip efficiency enhancement [40]. The round trip efficiencies of the CAES plants are around 54% in McIntosh, higher than 42% in Huntorf [22]. Additionally, other thermal energy recovery methods are also applied in the D-CAES system. It was reported that energy efficiency of a 100 MWe D-CAES can be increased from 48% to 86% by integrating a 105 MW thermal energy storage (TES) which was connected to a distinct heat network [41].

2.2. Adiabatic compressed air energy storage

Moreover, to eliminate the dependence on fossil fuels without a sacrifice of the performance of CAES, A-CAES is proposed. A-CAES systems use TES to recover and store the air compression heat during the compression process and reuses it at the expansion stage. As shown in Fig. 2(b), heat released from the state 2 to the state 3 is stored in TES and reused to increase the temperature of the air from the state 3 to the state 4. Compared to a D-CAES system, the energy input of A-CAES is only off-peak/renewable electricity. Thus, the round trip efficiency, which is the ratio of the electricity output during the discharge to the sole electricity input for the charging, is a key performance to evaluate an A-CAES system. In fact, in an A-CAES system, the off-peak electricity is stored in two forms, namely pressure of the compressed air and heat stored in the TES. Consequently, the storage and conversion efficiencies of both forms determine the round trip efficiency of the entire A-CAES system.

Efficiency of an A-CAES is expected to achieve 70–75% [23,42–44]. However, there is no commercially commissioned plants or projects that have demonstrated the expected efficiency until now. The performance of A-CAES varies with different designs. For instance, Grazzini and Milazzo reported an efficiency of 72% in a 16,500 MJ A-CAES system with variable configuration [44]. Garrison and Webber proposed a system using the A-CAES system that was driven by wind energy and concentrating solar power (CSP), and calculated the overall energy efficiency 46% for the CAES sub-system [45]. Using the ejector technology, performance of an A-CAES was improved by recovering the pressure loss. In the A-CAES system with an ejector, the system power output was increased from 31.10 MW to 32.81 MW and the round trip efficiency was improved from 61.95% to 65.36% [46]. Minutillo et al. used an small-scale A-CAES unit and a photovoltaic (PV) power system to supply a small-scale off-grid base transceiver station, in which the adiabatic operation was achieved by a TES unit to cool and reheat the air [47]. The efficiency of the small-scale A-CAES was reported to be > 50% [47]. ADELE project, an A-CAES system for electricity supply, undertaken by RWE Energy, expected to have an efficiency around 70% [48]. In China, Institute of Engineering Thermophysics, Chinese Academy of Science has built a 1.5 MW A-CAES pilot plant and constructing a 10 WM A-CAES pilot system, and relevant studies of the realistic performance of A-CAES are ongoing [49].

In fact, overall performance of an A-CAES is influenced by many factors from the charge to the discharge. Ke et al. studied the effectiveness and pressure loss of heat exchangers in A-CAES systems and found that the system efficiency of A-CAES can be significantly improved by increasing heat exchanger effectiveness either in the charge process or the discharge process [50]. Through analysing different CAES configurations, Hartmann et al. concluded that the key element to improve the efficiency of A-CAES is to develop high-temperature thermal storage (> 600 °C) and temperature resistant materials for compressors [51]. Barbour et al. proposed an A-CAES system based on direct contact packed beds as TES and suggested that an overall efficiency in excess of 70% is achievable [52]. In contrast, Wolf and Budt proposed a low-temperature A-CAES plant using multi-stage radial compressors and expanders, in which the temperature of the hot TES was 95–200 °C [53]. Although the proposed low-temperature A-CAES showed a slightly decreased round trip efficiency in the range of 52–60%, advantages of fast start-up characteristics and wide-ranging partial load ability were achieved [53]. Luo et al. carried out an examination of the potential system efficiency improvement using low-temperature TES in an A-CAES [37]. It indicated that the cycle efficiency and heat energy cycle efficiency of the designed low-temperature A-CAES systems can reach around 68% and 60%, respectively [37].

2.3. Isothermal compressed air energy storage

I-CAES is similar to Ericsson Cycle, and expected to have the highest round trip efficiency. In an I-CAES, the maintained temperature during the compression and expansion is capably achieved by the sufficient heat transfer using moisture in air or two-phase flow of air and droplets. The isothermal or quasi-isothermal process, therefore, leads to the least amount of thermodynamic work in compression and the maximum work of expansion. Kim and Favrat presented energy and exergy analysis of different types of micro I-CAES and A-CAES systems [54]. It indicated that quasi-isothermal compression and expansion processes are more preferable than adiabatic compression and expansion, especially for applications with high pressure ratios [54]. Excluding studies of the conventional volumetric expanders to achieve isothermal or quasi-isothermal compression and expansion [55–59], a concept of liquid piston whose structure is similar to reciprocating machines was proposed to improve the reversibility of gas compression and expansion [60]. The proposed liquid piston utilised a column of liquid to compress or expand gas in a fixed volume chamber, which is capable of maximising the surface area to volume ratio in the gas chamber, minimising the thermal dissipation, and creating the near-isothermal operation. The liquid piston was also reported to have no gas leakage, replacing the seal friction with viscous friction, and inherent thermal medium to carry and store heat [60].

To improve the isothermal operation for CAES, drop spray injection heat transfer was introduced and combined with the liquid piston [61]. Park et al. carried out an experimental analysis of the liquid piston for an ocean CAES prototype and demonstrated that heat transfer characteristics of the liquid piston compression were effective in reducing the air temperature and maintaining a near isothermal operation [62]. Saadat et al. also presented a novel I-CAES using the liquid piston for wind turbines [63]. Yan et al. carried out an experimental study on porous inserts of a liquid piston based I-CAES which had the pressure ratio of 10 for compression and 6 for expansion [64]. Besides using the liquid piston, moreover, enhancement of the heat transfer to maintain the isothermal compression and expansion is also achieved by injecting water spray or droplet into the air flow. SustainX used a mechanical link powering a two-stage, mixed-phase (water-in-air) heat transfer process within pneumatic cylinders [65]. The I-CAES power unit provided both isothermal compression and expansion. Another company, LightSail Energy, developed an I-CAES system by injecting a fine, dense mist of water spray which rapidly absorbs the heat energy of compression and uses it in expansion to maintain the constant temperature during the charge and discharge periods using reciprocating machines [66]. In addition to the reciprocating type of machines, studies of other types of machines to achieve isothermal or near isothermal compression/expansion are also found in literatures, such as screw [67] and scroll [68].

2.4. Operating conditions of D-CAES, A-CAES and I-CAES

The performance of the traditional D-CAES is determined by the maximum operating temperature according to the Carnot efficiency of heat engine. Conversely, for storage system with sole electricity input associated A-CAES and I-CAES, theoretically, their cycle efficiencies are

Table 2
Some CAES systems from literatures. [55,56,63,65,77,91–97].

Ref	System type	Temperature	Maximum pressure and minimum pressure in cavern/vessel	Efficiency
Huntorf CAES [89]	D-CAES	Maximum inlet temperature for LP is 850 °C, for HP is 550 °C	Maximum pressure is 7.2 MPa, Operation pressure 4.8–6.6 MPa	Round trip efficiency 42%
McIntosh CAES [73,91]	D-CAES with recuperator	Maximum inlet temperature is around 870 °C for LP, around 540 °C for HP	Operation pressure 4.5–7.4 MPa	Round trip efficiency 54%
[92]	D-CAES	Maximum temperature is 1050 °C Outlet temperature of LT 583 °C Exhaust temperature from HRSG 95 °C	Pressure 6 MPa	CAES-CC 51.1% Recuperated CAES 53.4%
[93]	D-CAES	Inlet temperature of HP is 550 °C Inlet temperature of LP is 827 °C Temperature of exhaust gas is 204 °C, Air temperature in cavern/vessel is 25 °C	Minimum operation pressure 4.2 MPa Maximum operation pressure 7.2 MPa	The second law efficiency is around 45%
[53]	A-CAES	Operating temperature is 90–200 °C	Two configurations considered: one is 7.2 MPa and the other is 15 MPa	Round trip efficiency 56%
[54]	A-CAES and I-CAES	Maximum temperatures for A-CAES are 623 °C and 239 °C for single-stage and two-stage compression, respectively; Maximum temperature is 80 °C for I-CAES systems for both configurations	Two pressure ratios: for single stage compression/ expansion the ratio is 50 (~ 5 MPa); for two-stage compression/ expansion the ratio is 7.1 & 7.1 (~ 5 MPa)	Round efficiency: A-CAES (single-stage) 23.6% A-CAES (two-stage) 48.6% I-CAES (single-stage) 70.6% I-CAES (two-stage) 73.9%
[75]	A-CAES	Maximum temperature 400 °C	Maximum pressure in cavern 6.6 MPa Minimum pressure in cavern 4.6 MPa	"hypothetically" 79.2% if heat exchanger effectiveness 0.7
[94]	A-CAES	Exhaust temperature 3 °C Air temperature at compressor outlet 159 °C Air temperature at turbine inlet 130 °C	Maximum pressure in tank 3.5 MPa Minimum pressure in tank 2.5 MPa	Storage efficiency is 57%
[95]	A-CAES	Maximum temperature ~ 150 °C Exhaust temperature 15 °C	Pressure ratio 90 (9 MPa)	Cycle efficiency is in a rage of 50–75% depending on stage number and turbine efficiency
[61]	I-CAES	Ideal isothermal constant temperature	Maximum pressure 1 MPa	More than 90%
[63]	I-CAES	Isothermal constant temperature Temperature difference less than 5 °C	Operation pressure 20–35 MPa	74.8% for entire wind and CAES system

independent of the maximum operating temperature and storage temperature [53]. The reported CAES systems, with their operation conditions and key parameters are listed in Table 2. As shown in Table 2, the highest operation temperature is found in D-CAES systems. In practice, the limiting temperature in D-CAES is restricted by the current development of compressors and expanders. Because of the availability of the proven gas turbine trains operating on a pressure drop of 11–1 bar, the air temperature at the inlet of the LP (low pressure) turbine can be as high as more than 800 °C [53]. Due to the high pressure drop of 42–11 bar of present HP (high pressure) gas turbines, D-CAES such as Huntorf plant, designed the HP turbine on "steam turbine engineering" practice [53]. As a result, the inlet temperature of the HP turbine is only 550 °C which is a common feature of current steam turbine operation. Detailed operational information of these two plants, Huntorf and McIntosh, can be found in [69].

In contrast, through the listed A-CAES system performance, it can be found a wide range of operating temperature, which is from 150 to 650 °C, approximately. The upper limit of the operational temperature is usually restricted by the availability and performance of high-temperature TES at present [70]. Taking advantages of the rapid development of the TES, especially the high-temperature TES, operating temperature is predicted to be increased. Until now, selections of the operating temperature and types of TES vary among different applications and groups. A reported project, the AA-CAES Project, is comprised of 19 different partners, considered a full range of thermal storage devices, including phase-change, high heat capacity solid and liquid media and hybrid systems. The project selected a range of solid media (natural stone, concrete, fireproof material and metal) as TES due to the advantages of high surface area for heat transfer and low cost of the storage materials [71]. But they also pointed out that expensive pressurised containers are required for solid TES [71]. Liu and Wang carried out a sensitive analysis of the heated temperature of the compressed air at the inlet of the HP turbines in the range from 490 K to 580 K using thermal oil as the sensible TES medium [72]. They found increased round trip efficiency and improved total exergy efficiency of the A-CAES [72]. Yang et al. summarised several sensible heat storage materials from literatures [73,74] and proposed a modified A-CAES system. They called the system hybrid thermal-compressed air energy storage using wind power, which further increased the temperature of heat storage (potential maximum temperature of TES was as high as 1273 K in their theoretical analysis) [75].

Compared to A-CAES integrated with the sensible TES, there is a limited number of published works of A-CAES using latent TES. Recently, Peng et al. studied an A-CAES incorporating Packed Bed Thermal Energy Storage (PBTES) filled with PCM particles [76]. Also, hybrid sensible/latent TES was proposed in the A-CAES systems using packed bed of rocks with encapsulated PCM on the top, in which the stored temperature was as high as 600 °C [77]. PBTES storing heat with sensible (solid particles) or/and latent heat (PCMs) is a promising and attractive method [78]. It has been investigated in solar thermal energy systems and energy saving buildings [79–81]. Tian and Zhao summarised and listed several commercial PCMs, inorganic salts and eutectics based on [82,83], which were listed in [84]. The phase change temperatures of these materials are ranged from 100 °C to 897 °C, and the latent heat is ranged from 124 to 560 kJ/kg. Therefore, the appropriate operational temperature of PCM shows the possibility of using the latent heat TES in the A-CAES systems in future.

In addition, the high energy density of latent heat storage will

reduce the required volume for storing certain amount of heat in an A-CAES system. The behaviour of near isothermal heat transfer of the appropriate PCMs during the phase change period is capable of significantly enhancing the heat transfer and optimally controlling the air temperature. Studies of PBTES with a cascade of PCM filling [85] further indicated the potential performance improvements with optimal PCMs-fillings in terms of selections and combinations of the different materials. However, PCMs usually have low thermal conductivities which needs to be improved by heat transfer enhancement technologies or new composite PCMs. For thermochemical TES, currently, there is no integration with A-CAES found in the survey of published literatures.

Moreover, as so called isothermal CAES, operational temperature from the charge to the discharge is supposed to be maintained constantly. However, due to the difficulties to achieve the isothermal compression and expansion processes, I-CAES systems are often operated at a near-isothermal operation. Slight temperature increases and decreases occur in the compression and expansion, respectively. From literatures, several operating pressures and temperatures are found in different experimental or/and theoretical I-CAES systems, which are shown in Table 2. Park et al. carried out a numerical analysis of a quasi-isothermal thermodynamic cycle for an underwater CAES and indicated only 26.6° increase of the final mean temperature with the air pressure increases to 25 bar [86]. In fact, Yan pointed out that a shorter compression/expansion time leads to a higher temperature rise and more close to the adiabatic process [87]. To overcome the trade-off, porous media inserts have been used to improve the heat transfer without the sacrifice of power density and thermal efficiency of I-CAES systems [88]. According to the computational results, the metal foam kept the bulk temperature below 360 K if it occupied the full chamber length (575 K for adiabatic as a reference) [88]. Also porous inserts increased power density by 39-fold at 95% efficiency and enhanced efficiency by 18% at 100 kW/m^3 power density in compression; in expansion, power density was increased three-fold at 89% efficiency and efficiency was increased by 7% at 150 kW/m^3 power density [64].

Apart from the operating temperature, operating pressures are slightly different for the three CAES systems as well. In a traditional D-CAES system, according to the integration of the gas turbine cycle and large volume of the cavern, the pressure of the compressed air can be adjusted to an appropriate value to meet the energy and power requirements during the charge and discharge periods. Conversely, because both A-CAES and I-CAES are usually used in the small-scale or micro-scale energy storage systems, such as the integrated CAES and wind turbine or other distributed energy generations, to achieve a high energy density of the storage and downsize the paired electrical components, high pressure of the compressed air is usually applied.

2.5. Further discussion of D-CAES, A-CAES and I-CAES systems

For choosing an appropriate system type, the functionality of the system determines the system type (i.e. D-CAES, A-CAES and I-CAES) and detailed configurations/specifications, such as the system rated power and energy capacity. The D-CAES and A-CAES systems are suitable for grid-scale energy storage applications (~ 100 WM and ~ 1000 MWh), and a small CAES system may choose the system type between A-CAES and I-CAES. Among the three system types, D-CAES systems have the highest degree of technology maturity and the lowest capital cost. However, D-CAES systems utilise fossil fuels in the operation and have emissions of carbon dioxide, nitrogen oxides, and sulphur dioxide. Nevertheless, D-CAES is still regarded as an energy storage technology with low environmental impact in general [96]. Depending on the local policies, potential penalties for these emissions will increase the lifecycle cost of the D-CAES systems. A-CAES and I-CAES systems have no burning fossil fuels involved and its realisation highly depends on efficient system configuration and expanders. A-CAES and I-CAES is still at the stage of pre-commercialization, so both the expected technical performance of the system and the cost-effectiveness need to be demonstrated.

High degree of reliability and stability of the system performance are the basic requirements for achieving the cost-effectiveness in a life cycle. With the operational data over decades, traditional large-scale D-CAES system has demonstrated its very high storage reliability and running reliability in both charging and discharging periods. Different from D-CAES, the reliability of novel A-CAES and I-CAES systems also depends on the performance of the heat storage and heat transfer effectiveness. High exergy capacity and low exergy loss of both the heat and gas storages are essential for these advanced CAES-TES systems.

Lifecycle economic cost of CAES is another crucial factor in determining the system selection. For grid-connected energy storage applications, as pointed by Budt et al., economic aspects are significantly determined by country-specific and short-term changing market conditions, and the political and regulatory framework [25]. For the off-grid micro-grid systems, the capital cost and the maintenance cost of CAES define the payback time of the systems. A cost-effective off-grid CAES system usually refers to a scenario in which the cost of the CAES system is comparable to other technology solutions. Because CAES systems have negligible maintenance cost, capital cost of the system dominate the life-time cost. Although the capital cost of a large-scale CAES system is usually high, the long lifetime and very little waste materials from the CAES system significantly decrease the detrimental effect of the high capital cost and result in a reduction of the system lifecycle cost. A major portion of the capital cost in these CAES systems is the high-pressure containment cost. White et al. assumed that the containment cost is proportional to the product of pressure, internal volume [97]. This pressure dependant containment cost governs the cost of vessel-based gas storage in all system types and high-pressure heat reservoirs used in A-CAES systems. Currently, Lightsail are trying to significantly reduce the cost by constructing the advanced carbon fibre tanks rather than using steel pressure vessels [98].

2.6. Other categories of CAES

Besides the classification of D-CAES, A-CAES and I-CAES, several novel CAES systems are also proposed in recent years, such as compressed air storage with humidification (CASH), underwater CAES (UWCAES), liquid air energy storage (LAES), and supercritical CAES (SC-CAES). In addition, replacing air with carbon dioxide, liquid carbon dioxide energy storage (LCES) are also found in literatures.

CASH is a gas turbine power plant based D-CAES combining air saturation to boost power and improve performance. A saturator is added in D-CAES and humidification is utilised to increase water vapour in the air flow. Because of the water vapour existing in the air, the recovery of waste heat which is used to heat up the mixture of air and water vapour results in an increase of up to 30% in energy per unit mass flow through the turbine without additional fuel and further compression [99]. In addition to efficiency increasing, emission of NOx formation is reduced due to the reduced combustion temperature [99]. Zhao et al. proposed a similar ideal that integrated the humid air turbine (HAT) cycle with D-CAES and built a combined heat and power system [100]. The power output of expansion train of the CAES-HAT was improved by about 26% compared to conventional D-CAES at the design operation [100].

UWCAES takes advantage of hydrostatic pressure and space of in deep water to build energy storage systems. In an UWCAES, compressed air is surrounded by water which is also acted as the pressure restraint. Thus, the pressure of stored compressed air is associated with that of the surrounding water's hydrostatic pressure. The storage volume of UWCAES usually changes during the charge and discharge processes, so a roughly constant pressure processes is maintained without the dependence on the remaining volume of air in the storage. Therefore, compressors and turbines are operated at their design operations all the time without loss of exergy of compressed air, leading to a high round trip efficiency (expected to be ~ 70%) and a high energy density

[101,102]. Based on the type of storage vessel used in UWCAES, two categories are classed: rigid vessels such as submerged caissons anchored to the seabed, and cable-reinforced fabric bags anchored to the seabed, usually known as Energy Bags [13]. Both approaches were studied respectively by different research groups worldwide [13,103–105].

LAES has very high energy density by storing compressed air in the liquid state, around 20 times higher than a normal CAES plant [106]. Usually LAES is suffered by low cycle efficiency which motivated the research for performance improvements. Several LAES systems are proposed and described by Ameel et al. [106]. The work showed that the cycle efficiency of the ideal Linde refrigeration and Rankine cycle to store liquefied air was 36.8% and 43.3% in the combined cycle using waste heat at 300 K Morgan et al. described a novel LAES by recycling and storing thermal energy between the charge and discharge processes, with 45% efficiency from a low grade heat to power [107]. Guizzi et al. also developed a study to assess the efficiency of LAES and indicated the obtainable round-trip efficiency in the range of 54–55% [108]. A LAES pilot plant (350 kW/2.5 MWh) has been built at Slough Heat and Power plant in London UK and a further scaled-up LAES pilot plant (5 MW/15 MWh) is being constructed in Manchester UK [109].

Alternatively, to increase the overall efficiency of CAES using liquefied air, SC-CAES is proposed recently. Without restrictions of current air liquefaction technologies, SC-CAES achieves a high overall efficiency due to advantageous properties of supercritical air [110]. In SC-CAES, compressed air is stored in the liquid state. The efficiency of SC-CAES can reach 67.41% and the energy density can reach 3.45×10^5 kJ/m^3, which is approximately 18 times larger than that of conventional CAES [110].

Rather than using air in LAES and SC-CAES, LCES uses carbon dioxide as working fluid to store energy in the liquid state. Compared to liquid air, carbon dioxide as working fluid has the advantages of high critical temperature and a susceptibility to liquefaction [111], which gives a flexibility in selecting material for cryogenic energy storage. Thermodynamic analysis of three energy storage systems using liquid carbon dioxide indicates the cycle efficiency in a range of 40–57% and energy density of approximately 36.061 kWh/m^3 [111].

3. Expanders: working principle, modelling approach and machine selection

Expander, in general, operates in a reverse process of the same type compressor. Various types of compressors are used in a wide range of applications, from fridges to rocket engines. These compressors have significant impacts on the prototypes of expanders. For compression and expansion, one is a reverse process of another, so key principles in design are shared between these two machines. Positive displacement machine mainly includes reciprocating type and rotary type in which screw and scroll are two of major expander types. In addition, dynamic machine is majorly divided into axial type and radial expander type. The positive displacement expanders are operated in an intermittent mode which is cyclic in nature. Conversely, dynamic expanders are operated continuously without interruption of the flow at any point in the expansion. Compared to expanders, as mentioned earlier, compressors are well developed and far more investigated. Typical operation ranges of these types of compressors are illustrated in Fig. 3, which are determined by their unique designs. Because of the similar design in geometry of expanders in the same type, these characterisations of performance can be considered to approximately characterise the same type of expanders in general.

3.1. Thermodynamic analysis and modelling of expansion process

Conventionally, thermodynamic analysis and modelling of a CAES is usually based on general compression and expansion process with ideal gas theory. The mechanical work of an expander is converted from

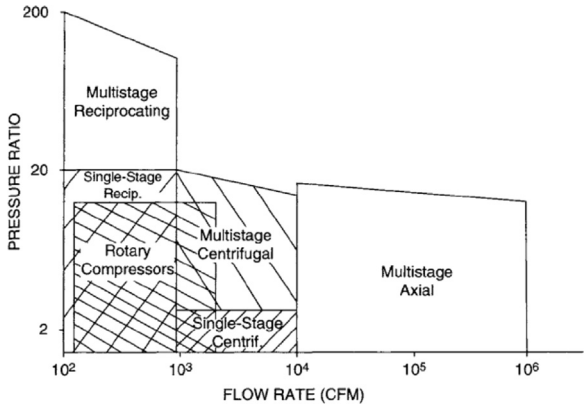

Fig. 3. Typical operational ranges of different compressor types [112].

energy change of compressed air. In accordance to the different expansion trajectories, enthalpy changes of air varies in different CAES system types. In both D-CAES and A-CAES, the expansion can be considered as isentropic processes without the heat transfer with external environment, or polytropic expansion when the heat transfer is considered with the environment. But expansions occurred in these two CAES processes have different initial conditions of the compressed air because of different inter-stage cooling and heating processes. Moreover, the isothermal expansion is maintained in an I-CAES system.

In thermodynamics, although these expansion processes are different, based on the first law of thermodynamics, expansions of ideal gas apply a general relation which is

$$pv^n = const \tag{1}$$

where n is an index which is varied among these processes: $n = 0$ for isobaric process, $n = 1$ for isothermal process, $n = \kappa$ for isentropic process, and $1 < n < \kappa$ or $n > \kappa$ for polytropic process. p is pressure of air, and v is specific volume.

The air enthalpy variations depends on the air expansion paths in expanders. The reversible specific isentropic expansion work of air can be expressed as,

$$\Delta h^s = \int_{in}^{out,s} \nu dp = \frac{\kappa}{\kappa - 1} R \ T_i \left[\left(\frac{p_{out,s}}{p_{in}} \right)^{\frac{\kappa-1}{\kappa}} - 1 \right] \tag{2}$$

where in and out present the initial and final state of the expansion, s presents isentropic process. T is temperature and R is gas constant, h is enthalpy. κ is the specific heat ratio. If the ideal gas equation presents air,

$$pv = R \ T \tag{3}$$

The temperature at the outlet of expander after the isentropic expansion can be also obtained,

$$T_{out,s} = T_{in} \left(\frac{p_{out,s}}{p_{in}} \right)^{\frac{\kappa-1}{\kappa}} \tag{4}$$

Additionally, according to the definition of polytropic efficiency, $\eta^p_{\exp}$, and the characteristics of polytropic process, the decrease of specific gas enthalpy during a polytropic expansion can be obtained

$$\Delta h^p = \eta^p_{\exp} \int_{in}^{out,p} \nu dp = \eta^p_{\exp} \frac{n}{n - 1} R \ T_{in} \left[\left(\frac{p_{out,p}}{p_{in}} \right)^{\frac{n-1}{n}} - 1 \right] \tag{5}$$

where superscript p presents polytropic process. The temperature at the outlet of the expander in a polytropic process is obtained replacing κ by n in Eq. (4).

Applying $n = 1$ in Eq. (1) and ideal gas equation as shown in Eq. (3), the change of specific air enthalpy from inlet to outlet in an isothermal expander can be presented as

$$\Delta h^t = \int_{in}^{out,t} v dp = R\ T_1 ln(\frac{p_{out,t}}{p_{in}}) \quad (6)$$

where t presents isothermal process.

Although air is usually treated as an ideal gas and this assumption has been widely used in analyses of CAES systems [37,51], realistic gas models increase the accuracy of predicting the expansion work and enthalpy change of air expansion through the expander in a CAES process. Budt et al. discussed effects of the real gas properties of air in CAES systems [25]. They used isobaric capacity as an example and illustrated how the real gas properties affecting the performance of an A-CAES system. The deviations of isobaric capacity between ideal and real gas models increase with an increase of pressure and decrease with a decrease of temperature. It indicated that the real gas behaves much differently as compare to ideal gas if the air is cooling down at a high pressure [25]. In addition, because water is actually contained in the ambient air, and water vapour might be injected into compressed air to increase the system efficiency (e.g. CASH); humid air is the working fluid of these CAES systems. Condensation of water vapour may occur during the inter-cooling in heat exchangers or flowing through TES, and appropriate real gas models of humid air should account for these behaviours, especially in high-pressure CAES systems. To this end, for purpose of more accurate predictions, a number of empirical correlations fitting experimental data of dry/humid air [113–117], have been implemented in the modelling to present the real gas effects. Software using these real gas models are also available, such as REFPROP [118] and CoolProp [119].

Compared to the general thermodynamic analysis, accuracy of the modelling can be significantly improved by considering the specific geometric design of expanders. Models of these expanders are important to characterise their operations and performance. These models are mainly classed into empirical, semi-empirical and geometry-based models. Empirical models are those purely derived based on experimental data. They are usually in algebraic expressions to present specific expander characteristics. These models can be easily evaluated without using iterative numerical methods. Therefore, empirical models are widely used in dynamic modelling at the system-level because of the low computations. Nonetheless, the parameters and expressions in the models are lacking physical meanings and only validated for restricted designs and operations. Additionally, semi-empirical models are developed. On one hand, these models usually consider the whole physical process of an expander through the inlet to the outlet. On the other hand, these models also involve parameters fitted by experimental data, such as energy losses. With the enhanced modelling accuracy, simulations using the semi-empirical models are slower than the empirical ones but still sufficiently fast to be integrated at the system-level.

In addition to empirical and semi-empirical models, geometry-based models, also called deterministic models, are based on geometric parameters of the expanders. Mathematical descriptions are developed on the basis of conservation laws of mass, momentum and energy to track flow changes through the expansion process including heat and mass (e.g. leakage) transfer. Fully resolved model in space refers to the computational fluid dynamics (CFD) which is a robust and powerful tool that accurately simulates the performance of expanders. However, compared to empirical models and semi-empirical models, computation of CFD modelling is extremely intensive, which takes much longer computation time. Therefore, they are primarily suited for analysis and optimisation of a well-designed expander, and not appropriate for dynamic simulations of expander over a range of operations at the system-level. To reduce the computational burden of geometry-based model, three dimensional models are simplified into one dimensional model with the averaged flow properties. These geometry-based semi-empirical models, therefore, are often used for the system-level modelling.

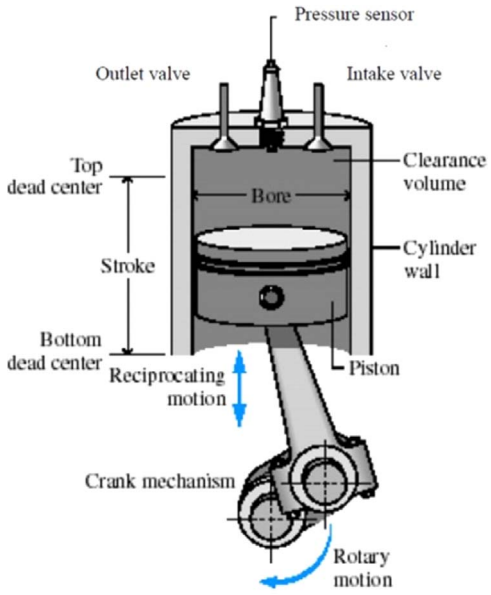

Fig. 4. An illustrated reciprocating machine's typical structure [120].

3.2. Reciprocating machine

The use of reciprocating machines as compressors/expanders is the patriarch of the family. The reciprocating compressor has a longest history in compressor development with wide applications ranging from households to industries. In general, the reciprocating machine is a volume-variation based, intermittent flow machine. The machine uses the reciprocating movement of piston within a cylinder to actuate gas from one pressure level to another (as shown in Fig. 4). The main component of a reciprocating machine consists of frame, crankshaft, crosshead, distance piece, piston rod, piston, cylinder, and valves. In a reciprocating expander, the compressed gas flows into the intake valve, and enters the cylinder where it is expanded by a reciprocating piston via a crankshaft. Gas is then discharged through the discharge valve. The potential energy of the compressed gas is transferred to mechanical energy of the shaft. In the expander, the timings of opening and closing the intake and exhaust valves can be controlled. For example, the intake valve of the expander opens when air reaches sufficient pressure in the cylinder. The air overcome the combined flow resistance of the valve spring load and the downstream pressure.

Reciprocating expander has low flow rate and high pressure ratio. The rotational speed is usually lower than that of rotary expanders, which is possible to avoid using speed reduction gearbox and the expander can be directly attached to the generator. Its isentropic efficiency is capable of being as high as 76% [121] but efficiencies less than 50% are also found [122]. For CAES systems, reciprocating expanders are appropriate for micro-scale and small-scale systems. In these scaled-down CAES systems, especially for micro-scale systems, because of the low storage capacity and low flow rate, relatively high pressures are usually necessary to increase the energy and power density. Reciprocating expanders are suitable for meeting these requirements in scaled-down CAES systems due to the high internal volume ratio that ranges from 6 to 14 [34].

Inheriting mature technologies from reciprocating compressors, reciprocating expanders can be directly modified and manufactured. The reciprocating expander, or piston expander, has been an interest in the 1970s with the development of car steam engines [123]. A reciprocating expander was studied in automatic waste heat recovery, tested in pressure ratios from 20 to 40, rotation speeds from 500 to 6000 rpm and up to 6 kW power output [124]. Wronski et al. optimised operations of a reciprocating expander for a medium-temperature heat source in an ORC system by controlling the condenser temperature and

the cut-off angle [125]. They found an isentropic efficiency approximately 90% of the expander over the large pressure ratios above 20 [125]. Oudkerk et al. experimentally tested a swatch-plate piston expander in an ORC system using R245a, and the designed piston expander was operated at the pressure ratio varying from 18 to 30 and the speed from 1000 to 4000 rpm [126]. A reciprocating expander was used in a Stirling Cycle to convert cryogenic energy to mechanical energy [127]. In addition, reciprocating expanders are more flexible to adapt for variable operations, and are more appropriate for directly connecting with the crank shaft compared to turbines [128]. Applications with low pressure ratios also use piston expanders [129,130]. Previous applications and studies on piston expanders in heat recovery Rankine cycle and internal engine have demonstrated the adaptability of the machine to tolerate moisture and two-phase flows [131,132], which indicated the technical viability of the reciprocating expander to be used in I-CAES. However, moving parts within a reciprocating expander make these machines high-cost maintenance and bulky. Existing clearance volume further reduces the intake flow rate and power output of the machine [133]. The novel liquid piston expander increases the energy/power density of storage by the improved heat transfer of the flow in a near isothermal process [134,135].

Reciprocating machines, require the modelling to consider the unique design of intake/discharge valves, piston, and cylinder. A simplified steady-state semi-empirical model of the reciprocating machine in refrigeration was proposed first in compressor, which consists of five consecutive processes to represent the air flow: pressure drop due to the supply throttling, heat-up due to heat exchanges between suction gas, discharge gas and the ambient, isentropic compression, complementary cooling-down near the discharge valve and pressure drop through the discharge valve [136]. Seven input parameters were used in the model: a swept volume parameter, a clearance factor, two throttling parameters for the two valves, three heat transfer coefficients and two shaft parameters. The same model was also applied in [137], and another similar model was found in [138].

Inspired by these models of reciprocating compressor, models of the expander were developed. According to Glavatskaya et al.'s work [124], the scheme of the overall expander model consists of several consecutive steps, as shown in Fig. 5(a). The expanded fluid in the expander encounters a series processes, including pressure drop (su to su,1), cool-down (su,1–su,2), internal expansion due to volume variation (2–3), under or over expansion (3–4), heat-up (ex,3–ex,2) and pressure loss at the outlet (ex,2–ex,1). In addition to these processes, internal leakage (su,2 to ex) and clearance flow (5–6–1) also exist. As a consequence, an operation cycle of the reciprocating expander is simulated by assembling all the processes, as shown in Fig. 5(b). To more accurately consider the heat transfer, Mathie et al. pointed out the unsteadiness of heat transfer as the piston moves periodically [139]. They proposed an one-dimension framework of unsteady and conjugate heat transfer in the presence of displacement work, and evaluated the fluctuating unsteadiness of heat transfer [139].

3.3. Rotary expander: screw and scroll expander

The rotary screw expander (twin screw) usually consists of two intermeshing helical rotors contained in housing, as shown in Fig. 6(a). The expansion is achieved by the intermeshing of the two motors. In a screw expander, the main rotor is driven by the compressed gas flow. The other rotor is driven by the main rotor with or without oil injection. As the rotors rotate, gas keeps entering the expander due to the increase of the intermesh space. When the specified intermesh space is fulfilled, the rotation of the rotors expands the gas with the increase of the interlobe space and moves the gas toward the discharge port. The volume of the gas is progressively increased and the pressure is reduced. Finally, further rotation of the rotors uncovers the discharge port, the exhaust gas flows out the expander and starts a new cycle. In addition to the twin screw, single screw machines as illustrated in Fig. 6(b) are also used in compression/expansion. It generally utilises one rotor and two gate-rotors to fulfil the intake, compression/expansion and discharge processes. The physical arrangement of the porting and rotors' design significantly influence the performance of a screw machine. The length and diameter of the rotor pair determine the flow rate and pressure ratio of the machine. Usually, a longer-rotor results in a higher-pressure ratio; a larger of the rotors' diameter causes a larger the screw capacity.

Compared with reciprocating expander, pressure ratios of screw expanders are usually lower due to the decreased built-in volume ratios. The reported power output of screw expander varies from 1.5 kW to 1 MW [140,141], and the isentropic efficiency varies from 20% to 70% [142–144]. As rotary expanders, screw expanders usually have higher rotational speed than reciprocating expanders, and hence, screw expanders might require the speed reduction gearbox to match the speed of the generator. In addition, screw expanders allow two-phase working fluid, which is appropriate for I-CAES. However, screw expander is not recommended for the capacity less than 10 kW because of the leakage losses and difficulties in manufacture [34,145]. The internal leakage of screw expander can be classed into two categories [142]: the leakages between adjacent expansion chambers and the ones between expansion

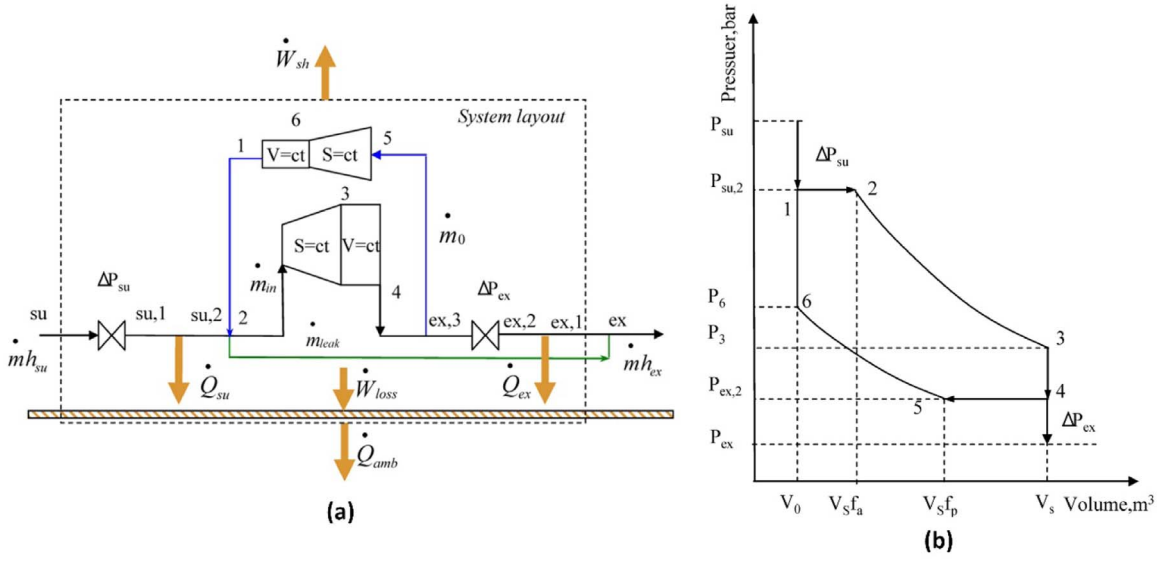

Fig. 5. Schematic representation of the overall expander model in (a) and PV diagram representation of the internal expansion process in (b) [124].

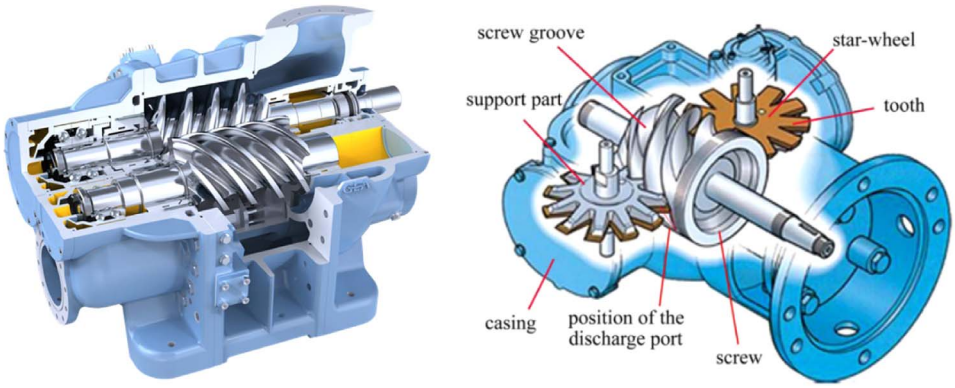

Fig. 6. Twin screw machine from Eltacon Engineering BV Gas Compressor Packages (http://www.eltacon.com/?m_id=31&lang=en&t=ELT_Gas_Compressor_Packages, accessed in Jan, 2016) and single screw machine [146].

chambers and discharge port. Design and optimisation of the rotors' profiles are important to reduce the leakage and frictional losses.

For applications with small power capacity, scroll expanders are usually preferred. The scroll machine is based on the fundamental design which is made up of two identical involutes, the orbiting scroll and the fixed scroll as shown in Fig. 7. In a scroll expander, as the orbiting scroll is driven by compressed air and moved around the fixed scroll, the pockets are formed by the meshed scrolls due to the involute spiral during the rotation. Air flows to the intake chamber at the centre of scroll expander. With the move of the orbiting scroll, the meshed volume between the two scrolls which is expansion chamber increases, and the pressure of the compressed gas decreases. Further rotation of the orbiting scroll, finds the discharge port and discharges the exhausted gas in the exhaust chamber. Although scroll expanders have advantageous performance of small machines compared to screw expanders, the limiting size of the scroll is also restricted by several factors. Leakage path of a scroll, which is at the apex of the crescent shaped pockets, restricts how small a scroll machine can be as a function of pressure ratio. Additionally, the upper limit of a scroll size is constrained by the maximum centrifugal force generated by the orbiting scroll in a large scroll machine because of the centrifugal force increases quadratically with respect to the scroll diameter. Compared to screw expanders, pressure ratios of scroll expanders are usually lower due to the reduced built-in volume ratios that are usually in the range of 1.5–5 [147,148]. As a volumetric expander, under and over expansions occur when the internal volume ratio is lower or higher than the specific volume ratio required by the pressure ratio.

In last decade, many studies including both experimental and numerical works were conducted for rotary expander applications,

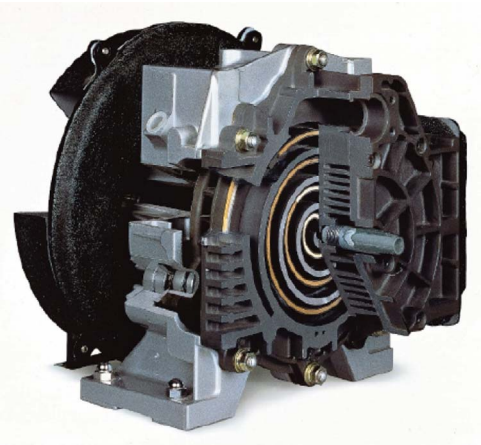

Fig. 7. Scroll machine from Atlas Copco. http://www.atlascopco.co.uk/ukus/products/air-and-gas-compressors/1473291/1516773, accessed in Dec 2015.

because of the advantages of less moving parts, simple structure, low cost and ease in restructure from the compressors. A single screw expander which has 1–200 kW range of power output was designed by He et al. and the machine achieved an optimum efficiency of 55% with the tested intake pressure from 4 to 16 bar [149]. Ziviani et al. analysed a 11 kWe single-screw expander with built-in volume ratio 4.7 [150]. Desideri et al. modified a single screw compressor with the built-in volume ratio of 5 into an expander, and measured the maximum power output of 7.8 kW at 3000 rpm with isentropic efficiency 64.7% and pressure ratio 7.7 [151]. Xia et al. studied experimentally the effect of the inlet fluid condition on the pressure ratio and the efficiency of a single-screw expander [143]. Stosic et al. showed how the rotor forces created by the compressor/expansion were partially balanced to eliminate the axial forces and reduce the radial bearing forces in high-pressure applications with the twin screw machines [152]. Tang et al. studied a twin screw expander both experimentally and theoretically considering effects of rotation speed, intake pressure and inlet preheat [153]. The results indicated that the isentropic efficiency of the expander decreased from 88% to 60% and the volumetric efficiency decreased from 88% to 70% when the rotational speed increased from 1250 to 6000 rpm [153].

Among studies focusing on scroll expanders, Clemente et al. modelled two scroll expanders with different built-in volume ratios, and demonstrated that the entire operational field of the expander moved to high pressure ratios when the expander with a higher internal volume ratio [147]. Peris et al. further experimentally tested the appropriate pressure ratio of a scroll expander with a built-in volume ratio of 8 in an ORC system, and found the pressure ratio around 7 was the optimum to achieve the maximal isentropic efficiency 65% using R245f [154]. Declaye et al. presented the experimental characterisation of an open-drive scroll expander with the internal volume ratio 3.95, the power output 2.1 kWe, and isentropic efficiency 75.7% in an ORC using R245fa [32]. A 2.1-wraps scroll air motor with the supply pressure around 4.4 bar was used in a hybrid wind turbine and CAES system [155]. Sun et al. also used a scroll expander that was modified from Sanden TRSA090 compressor in a hybrid wind turbine, and the CAES system with the inlet pressure around 5 bar [156].

Rotary positive displacement expanders are appropriate for applications with higher flow rates and lower pressure ratios than reciprocating machines. Belonging to volumetric expanders, rotary expanders, such as screw and scroll expanders, are also tolerable for moisture and two-phase flows, which make these machines are suitable for I-CAES systems as well. A comprehensive review of methods in affecting the quasi-isothermal expansion has been carried by Igobo and Davis, in which liquid flooding has been identified for primary use in rotary expanders [157]. Iglesias and Favrat presented the theoretical and experimental development of an oil-free co-rotating scroll air compressor and expander working with water injection in an I-CAES

system [158]. Further compared to reciprocating expanders, both screw and scroll expanders have potential advantages of lighter weight, less noise and pulsation within operations. Rotary machines have negligible clearance volumes and higher efficiencies at the same specific speed than reciprocating expanders, according to the unique design in which the intake, expansion and discharge occur in different space. Another advantage is that rotary displacement machine not only has similar efficiency to the single-stage turbine but also lower rotational speed and smaller size. Therefore, rather than turbines, rotary expanders are usually more suitable for micro-scale and small-scale CAES systems.

To predict and estimate the performance of these two rotary expanders, in the last century, a number of analytic models were developed to study the thermal performance [159,160]. In recent several decades, numerical modelling were also important approaches to design and predict performance in operations. Excluding CFD based studies, empirical models and semi-empirical models are most widely used tools. Avadhanula and Lin developed an empirical model of screw expanders in which the polytropic process with a curve-fitting polytropic index was assumed based on experimental data [161]. Ziviani et al. presented a detailed geometry-based model of a single screw expander [162]. The model used a rotation-dependant function and calculated the swept volume at every angular step with the inlet conditions [163]. The model was validated with experimental data and demonstrated the error within ± 10% and ± 15% for prediction of mass flow rate and power output [163].

Moreover, since scroll type of expander is a relatively new member in the family of expanders, few models were developed to simulate the process. A semi-empirical scroll expander model was developed by Lemort et al. [30] based on the reverse operation of a validated scroll compressor model [164]. Quoilin et al. used the model to simulate an actual ORC system and compared the results between simulations and experiments [31]. The comparison between the predicted values and the experimental results showed a fairly good agreement [31]. Since then, these validated steady models have been widely used as the basis in various applications using the scroll expander [165–167].

Lemort et al. proposed a general semi-empirical model to simulate both screw and scroll expander with different characterised parameters, such as internal volume ratio, swept volume, leakage area, intake area etc. [34]. The schematic representation of a rotary expander model is shown in Fig. 8. According to the model, the evolution of the fluid through the expander is decomposed into several consecutive processes [30]: adiabatic supply pressure drop (su-su,1), isobaric supply cooling down (su,1-su,2), expansion due to internal volume variation (su,2-ad), under or over expansion due to unbalanced pressure ratio and internal volume ratio (ad-ex,2), adiabatic mixing between supply and leakage (ex,2-ex,1) and isobaric exhaust cooling-down or heating-up (ex,1-ex).

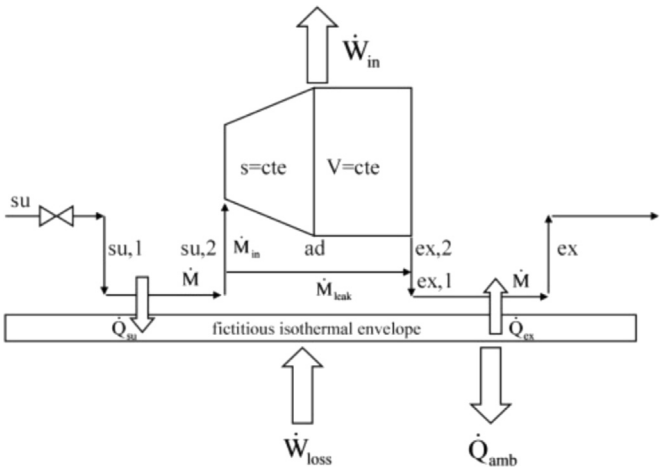

Fig. 8. A schematic representation of a general rotary expander model [30].

Compared to the model of piston expanders shown in Fig. 5(a), the rotary expander model does not consider the effect of recompression of gas in the clearance volume, because of the negligible clearance volume in both screw and scroll expanders. The model was proposed for scroll expander in [30] and used to evaluate the operational map of both screw and scroll expanders with different volumetric flow rates, internal volume rates and isentropic efficiencies in [34].

Liu et al. developed a geometry-based model describing the working process of scroll expanders and predicting its performance [168]. The model was based on mass and energy balance through the revolution of the rotating angle, which is capable to present the variation of the air flow due to the changing volume in a cycle. The model easily couple with mechanical model and load resistance model, and simulate the expander-generator system [169]. For dynamic modelling of scroll expanders, Wang et al. developed a complete geometry-based mathematical model for dynamic analysis of scroll energy efficiency and the influential factors [170]. Detailed derivation of spiral equations, chamber volume calculations, the driving torque of the scroll expander and the evolutions of the air thermodynamic properties were developed with respect to the rotating scroll in the operation [171].

3.4. Turbomachines: radial and axial expander

Radial machines belong to the class of dynamic machines in which conversions between rotational kinetic energy of the impeller and thermodynamic energy of the fluids occur. Radial expander, usually referring to the radial-inflow turbine, has reversed gas flow and opposite rotation compared to the centrifugal compressor. Compressed gas flows into the stator/nozzle through the scroll of the turbine, in which potential energy of gas is converted to its kinetic energy. The enhanced kinetic energy of gas drives the impeller rotating, and the expanded gas usually exits the impeller axially. An advantage of the radial-inflow turbine is that the work produced by a single-stage is approximately equal to that of two or more stage of an axial turbine. This is a result of the larger size of the impeller with the high tip speed difference between the inlet and outlet of the impeller (Figs. 9 and 10).

To place radial turbines in the family of expanders, on one hand, compared to the volumetric expanders introduced above, turbines usually allow higher flow rates but lower pressure ratios through a single-stage. Higher flow rate is achieved due to the continuous operation in turbines without intermittent operational variations during the expansion. On the other hand, compared to axial turbines, radial turbines are suggested to elaborate higher pressure ratio and lower flow rates, whose power output from a few kilowatts up to a few Megawatts [172].

For a plant whose scale is larger than ~ 10 MW, axial turbines are preferred. Axial turbines also belong to the class of dynamic machines. Axial machines are characterised to be high-speed. Although the pressure ratio of an axial machine is less than that of a single-stage radial machine, its capacity can be considerably large. As named axial machines, the gas flows in the axial direction within the machine. An axial turbine generally consists of a rotor, a stator, and a cast. An additional inlet guide vane might be used to change the inlet angle. Axial turbines are the most widely employed turbines in existing power plants to generate electricity. Steam turbine is a device to generate rotary motion of the rotors from the thermal energy of the pressurised steam. The rotary motion of the shaft drives an electrical generator to produce electricity. Gas turbine is another application of turbines in power generation with air as the working fluid. Fresh air flows through the compressors for increasing the pressure. Energy of the air is further increased by spraying the fuel into the air and igniting the mixture. As a result, combustion generates the high-pressure and high-temperature air flow, which produces the mechanical work in axial turbines. Industrial gas turbines closely integrate with the electrical generators and the secondary energy recovery device to recover the waste heat, such as heat recovery steam generator (HRSG).

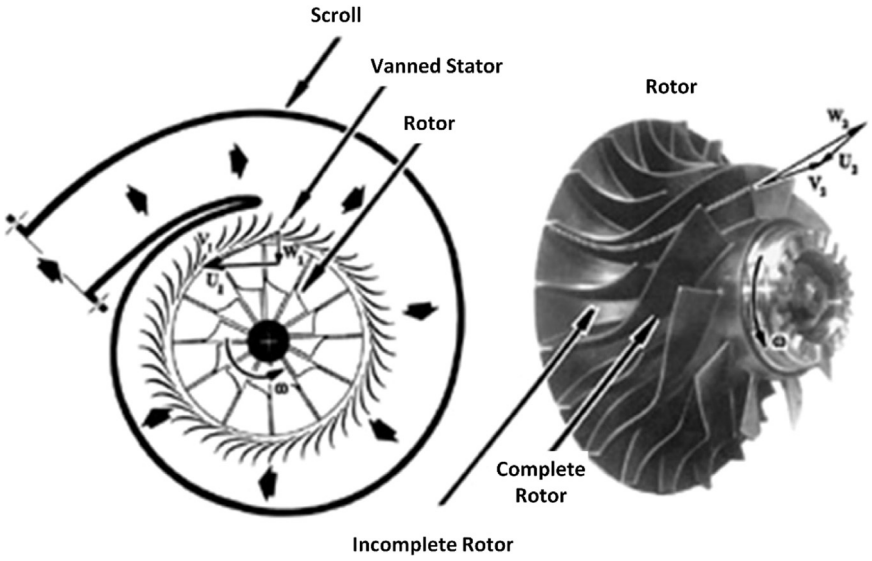

Fig. 9. An illustrated radial turbine [173].

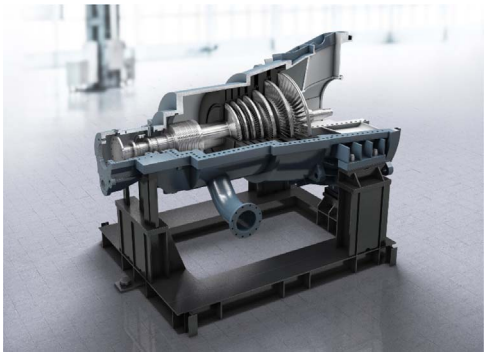

Fig. 10. Axial steam turbine from SIMENS. http://www.siemens.com/entry/cc/en/, accessed in Dec 2015.

Turbomachines have been utilised in existing CAES systems, especially in large-scale systems. Generally, operational window of turbomachines locates at high rotational speeds, which are far above the operation speeds of positive displacement machines. Large flow rates, low pressure ratios, and large machine sizes characterise turbomachines' performance and geometries. Because of the difficulty to deal with the moisture and two-phase flow, turbines can hardly be used in I-CAES systems. Theoretically, turbines used in D-CAES and A-CAES systems have no obvious difference from turbines used in power plants. However, the different operating temperature of the compressed air at the inlet of turbines significantly affects the turbines designs and performance. Mature technologies of turbines are translated from gas turbine cycle and Rankine cycle to large-scale D-CAES and A-CAES systems, including multi-stage turbine-train with HP, MP and LP turbines, but the specifications of turbines need to be modified for fitting the operating conditions of CAES. For example, high-pressure and high-temperature CAES systems, such as SC-CAES, should be modified to reduce the pressure drops.

Additionally, utilisation of turbines also exists in small-scale energy recovery systems. As the distinctive characteristics between axial turbines and radial turbines, radial turbines are more attractive in small-scale CAES systems. Sauret and Rowlands pointed out several advantages of radial turbines over axial turbines [174]: 1) capability of maintaining high efficiency levels in off-design conditions through the inlet guide vane; 2) high efficiency at small sizes due to the less sensitive to blade profile inaccuracies of radial turbines; and 3) easy to manufacture. Several realistic radial inflow turbines were designed for ORC, ranged from 254 kW to 338 kW of power output with the efficiency at approximately 77% [174]. A 50 kW radial turbine was designed for six working fluids in an ORC system and the possible rotor diameter was 50–80 mm, with a rotation speed ranged between 32,000 and 55,000 rpm and the efficiency within 78–85% [175]. Kang designed a radial turbine coupled with a high-speed generator using R245a in ORC, with pressure ratio 4.11, isentropic efficiency 78.78% and power output 32.7 kW [176]. A range of pressure ratios of single-stage radial turbine are between 1.1 and 6 according to the review work carried out by Bao and Zhao [29], with power output from 0.15 to 33 kW. The principles to design these radial turbines can be utilised in designing radial turbines in small-scale CAES in future but considering working fluid with compressed air.

To estimate the performance of dynamic expanders, the simplest approach is characterising the turbine as an adiabatic nozzle of a given effective flow area, which was presented by Watson and Janota in studies of turbochargers [177]. The representation of the turbine as a nozzle presents the pressure drop for a specific mass flow rate. However, the ability of predicting the inlet and exhaust manifold pressure is limited, because of the lower expansion ratio of the shock occurred in a nozzle compared to that in high reaction turbines. As the expansions occur in both stator and rotor, the critical flow conditions are overestimated to higher expansion ratios. Another drawback of this model is that the effective throat area of the nozzle is assumed to be constant, which is inaccurate with respect to different expansion ratios. Therefore, an alternative to this assumption was to set a changing effective area and altered the pressure drop generated in the turbine [178,179]. Furthermore, a turbine model based on two nozzles in series, separated by an intermediate reservoir with the same volume to the turbine was proposed by Payri [180,181] and Baines et al. [182]. The assumption combined the advantages of the previous similar models and solved the problem associated with high expansion ratios. The existence of the intermediate reservoir allowed mass accumulation in the volume, and accounted for emptying and filling of the turbine's internal volume in dynamic modelling [183].

Another approach of empirical modelling is to use the experimental performance curves, such as maps of mass flow rate and efficiency, to simulate turbines. With the experimental data provided by the manufacturers, simulations and predictions of the unknown mass flow rate or/and efficiency of the machine are accomplished by interpolating and extrapolating of the experimental map [184]. This experimental data based approach can be extensively used, relying on the similarity concept from dimensionless analysis [185]. However, for inclusion of

performance map and look-up table into system simulation models, several drawbacks of the model usually exist. For example, the performance maps and look-up tables are possibly inapplicable or not well-suited for the studied cases. Standard interpolating methods are not continuously differentiable, making it difficult to validate the accuracy of the model. Extrapolation is unreliable based on the experimental data of the limited operational points. To this end, good empirical models require a large quantity of experimental data and cover full range of operations. Some of these models can be found in [186–189]. Fang et al. carried out comprehensive reviews of these empirical models for efficiency and mass flow rate, including both turbines [190] and centrifugal compressors [191].

Compared to volumetric expanders, flows in turbines are complex and strongly three-dimensional because of the high Reynolds numbers. Consequently, to describe the internal flow within the turbines and optimise the blade profiles, several numerical flow models were developed subject to the computation resources available. In 1950's, in order to reduce the computation time, Wu proposed an unified approach called general non-orthogonal curvilinear method, deriving the governing equations by using two stream functions and non-orthogonal coordinate systems. This new set of equations at that time allowed accurate calculation in both the inverse and direct turbomachinery problems for any arbitrary geometry, with significantly less computation than the fully-resolved CFD modelling [192]. Two dimensional methods using empirical correlations or assumptions to simplify the energy, momentum and continuity equations, reduced the execution time as well. The flow dimension was reduced with the given pressure evolution in the flow direction or in the span-wise direction [193]. However, this two-dimensional model is still challenging to be used in system-level modelling.

One dimensional model of turbines, usually known as the mean-line model, solves the velocity triangles along the flow path incorporating empirical losses models to predict the performance of turbomachines. Thus, the model is referred as one of the geometry-based semi-empirical models, combining physical modelling and empirical modelling. The triangle velocity calculation is based on the key geometric parameters of rotor and stator. Energy losses are related to aerodynamics of gas flowing through the turbine. This method is also known as Euler Equation of Turbomachinery. The representations of velocity triangles at the inlet and outlet of the rotor are shown in Fig. 11, in which both radial type and axial type are included in (a) and (b), respectively. Due to simplicity of the model, the computation cost is significantly reduced, making the model applicable to be used in dynamic modelling, diagnose and control at the system level. However, as the existence of the empirical parameters in the loss models, predictive accuracy necessitates model calibration with experimental data.

Rahbar et al. used the mean-line modelling to investigate the effects of key input parameters, including velocity ratio, rotational speed and rotor flow angles at the turbine rotor inlet, on the overall performance [194]. Hu et al. used the mean-line models of the radial turbine and studied the performance in off-design operations with the energy losses models [195,196]. A comprehensive review of the loss models was carried out by Oh et al. [197] and they also summarised an optimum set of empirical loss models for a reliable performance prediction of dynamic machines [197]. A project was carried out by Persson to validate two 1D turbine design tools, AXIAL by Concepts NERC and YML by GKN Aerospace using the KTH Test Turbine [198]. The project proved the ability of the 1D modelling tools to simulate the performance of the single-stage with high pressure ratios in a reasonable degree of accuracy, but the results were below satisfactory from a validation stand point at low pressure ratios [198]. It also pointed out that the unsatisfactory performance of the 1D model might be caused by the inappropriate selection of loss models [198]. Therefore, the conclusion of the project was that 1D simulation could still be a viable tool for preliminary turbine design and simulation in competition with advanced approach (e.g. CFD) [198], but good knowledge of specific 1D model and appropriate loss model is essential to reach a significant degree of the accuracy in modelling [198]. Kacker and Okapuu described a mean line loss model to predict the design point efficiencies of axial gas turbines, and tested the model using 33 turbines which efficiencies were known [199]. Predicting accuracy of the efficiencies of a wide range of axial turbines were ± 1.5% [199]. Lio et al. developed a mean line design procedure of the single-stage axial flow turbine [200]. The method was successfully applied in designing turbines in ORC systems with different critical temperatures (from 367.9 K to 511.7 K) [201].

4. Selection suggestions for expansion machines

From the review of expander types and applications, it is found that the performance of expanders are significantly affected by the operations and thermodynamic property changes of the working fluid. A good systematic selection guidelines for expansion machines is highly needed to achieve whole CAES system efficiency. As overviewed in the previous sections, CAES has several different system configurations, various structures for operations and the range of scales in the applications serving different purposes. Although it is not realistic to have a

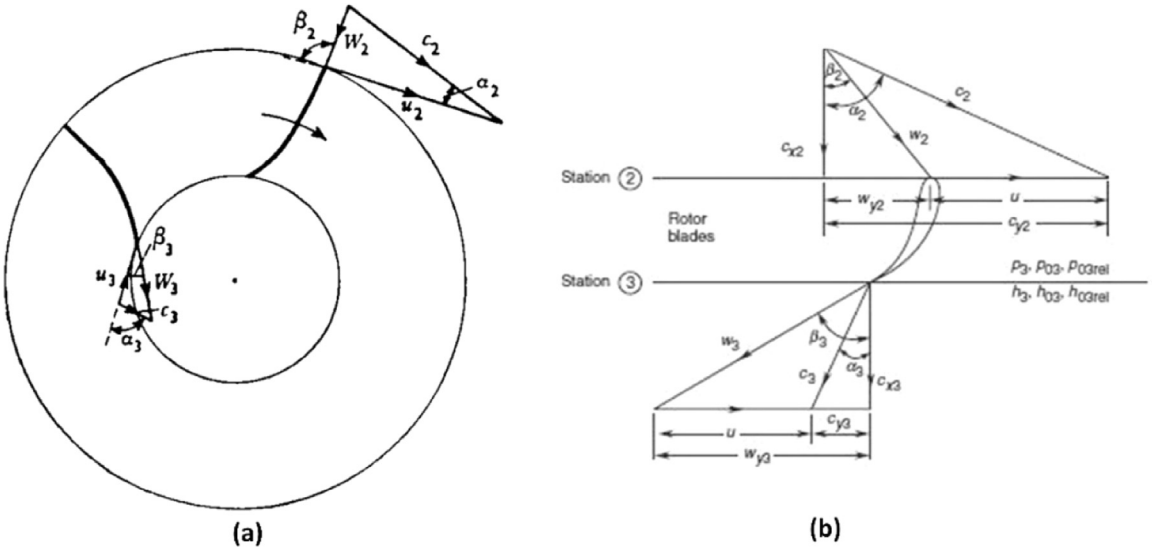

Fig. 11. Velocity triangles for a turbine stage. Velocity triangles of a radial rotor is shown in (a) [90] and velocity triangles of an axial rotor is shown in (b) [202].

standard procedure in selection of air expanders, the paper gives the following suggested generic procedure as a reference for CAES system,

- Step 1: understanding the CAES system, and configuring the air-expansion stage number and inter-stage heating numbers of the air expansion;
- Step 2: detailed operations of the expanders, which include the air being handled, input and output pressures, input temperature, air flow rate, etc.;
- Step 3: calculations of the selected expanders' specifications.

The selection of appropriate expanders is relevant to system scale, system types and operating conditions. At the system-level, the expansion stage-number refers to the number of expanders connected with the shaft in series, and the number of inter-stage heating is the number of heat source/storage used for heating up the air before expansion. The air-expansion stage-number is determined by the discharging pressure in a CAES system. If the discharge pressure of air from the gas storage is fixed, air expansion work generated theoretically increases with the inter-stage heating. However, the enhanced pressure losses, extra economic cost, and system complexity also increase. Therefore, an optimal stage-number need to be compromised in between the expansion efficiency and economic cost.

In a conventional D-CAES system, due to the additional fossil fuels involvement, high power generation is achievable during the air-expansion. As a result, these systems usually not fully utilise the air pressure to produce electricity that the compressed air usually is expanded to a pressure higher than the atmosphere pressure with the exhaust heat. Plants such as Huntorf and McIntosh (air pressure in the cavern $>$ 46 bar), have two-stage air-expansion, including a HP turbine train and a LP turbine train. In the D-CAES system with the low-pressure air storage ($<$ 12 bar) [203], a single-stage LP air-expansion train was used, and the single-stage high-temperature (900 °C) heating was achieved through cascaded solar heating and combustion. In an A-CAES system without fossil fuels, the efficiency of air-expansion becomes crucial and both the energy from the compressed air and the stored compression heat need to be sufficiently utilised. In the A-CAES system with in-direct heat exchanges and sensible storages, the number of inter-stage heat exchangers is usually equivalent to the air-expansion stages, as the low-temperature A-CAES systems reported in [37] and [53]. Similar to the multi-stage compression with inter-stage cooling, the stage-number of the air-expansion is a result of minimising exergy losses in the air-expansion and pressure losses of flow in pipes and heat exchangers. The recommended stage-number in terms of overall expansion ratio can be found among different expander types in [204–206]. In [207], an A-CAES system with 500 kW discharging power rating, 2.5 MPa discharging pressure, and the heat storage of 110 °C pressurised water was built, tested and investigated. A three-stage expansion with the pressure ratios 2, 2.8 and 3.9 was designed to fully expand the compressed air to the atmosphere pressure. In A-CAES systems with direct heat storage such as PBTES, the number of inter-stage heating is restricted by the number of PBTES used in the compression. In an A-CAES system with the direct heat storage as reported in [208], the single inter-stage heating was placed before the HP turbine train, because there was only one PBTES tank in the system for storing the compression heat. While a two multi-stage turbine trains, HP and LP turbine trains, were used to expand the compressed air from the discharging pressure 46–1 bar [208].

From the above analysis, recommendations of selecting expansion machines are drawn in Table 3, which is subject to CAES system types and scales. When an application of CAES is specified, expanders can be preliminarily selected. In fact, there are overlapped operational ranges of expansion machines so there might be more than one options available for the CAES application specified. For example, the capacity of volume based expanders becomes large to extend the operation power range, and the radial turbines tend to progress with high efficiency while working in the systems with the power less than 100 kW. Selection of expansion machines also needs to consider other influential factors subject to the availability, such as lubrication requirement, leakage, dynamic vibration, reliability and cost.

Once the configuration of CAES has been established, the type of expander needs to be selected before the specifications are drawn. The type of expanders can be specified using the diagram of specific speed and specific diameter relationship in Fig. 12. This general approach to describe an expander was proposed by Balje, which was based on the concept of similarity in design of turbomachinery [209]. According to the method, four dimensionless parameters, Reynolds number, Mach number, specific speed and specific diameter, are used to describe the performance of geometrically similar expanders. For an expander with a particular flow rate and a pressure ratio, specific speed is an indicative parameter related to the rotation speed of the machine, and specific diameter is depending on the diameter of the rotor or the size of the displacement machine. Reynolds number is the ratio of inertial force to the viscous force. Mach number is the ratio of the flow speed to the local sound speed, which reflect the properties of the fluid being pumped/compressed and the speed of the machine. Latz et al. indicated that Reynolds number and Mach number of the expanding fluid have only secondary effects on expander's behaviours [210]. In other words, on the basis of machine's geometric type, the performance can be estimated only with operations and machine sizes. Originally, specific speed was applied almost exclusively to dynamic machines for selecting the optimum type and size, and Balje extended the method to volume-based machines [209]. For both volumetric and dynamic expanders, the performance of the expanders can be estimated as functions of the specific speed N_S and the specific diameter D_S, which are

$$N_S = \frac{N V_{ex}^{1/2}}{\Delta h_s^{3/4}} \tag{7}$$

$$D_s = \frac{D \Delta h_s^{1/4}}{V_{ex}^{1/2}} \tag{8}$$

where V_{ex} is the volumetric flow rate of fluid at the exhaust port, N is the rational speed, and D is the characteristic diameter.

The volumetric flow rate is obtained through the CAES system's specifications and the equation of state (Eq. (3)). With the selected rotational speed, the specific speed is estimated. The diameter of the expansion machine that achieves a certain enthalpy drop is approximated by the assumed volumetric efficiency of positive displacement expanders or the polytrophic efficiency of turbines. Moreover, more geometric parameters are designed for the expanders using empirical or/and semi-empirical relations. A figure that illustrates the generic design procedure with both system-level and component-level considerations is plotted in Fig. 13.

In the preliminary design loop, constrains and restrictions present in all types of the expander designs. For example, the displacement expanders with a large swept volume and volume ratios highly possible have leakage issues and significant vibrations. Quoilin et al. pointed out that the maximum internal built-in volume ratio of rotary expanders is usually no superior than 5, which is limited by the length of rotor in a screw expander and by the number of spiral revolutions in a scroll expander [211]. Internal volume ratios for reciprocating expanders are larger than those of rotary expanders. The ratios between 6 and 14 are usually achievable, but the maximum ratios are restricted by the specific work of the machine and the compactness of the design [34]. The flow rates of the volumetric expanders are limited by the swept volume. According to [34,211], typical displacements of reciprocating expanders are ranged from 1.25 to 75 L/s, those of screw expanders are ranged from 25 to 1100 L/s, and those of scroll are ranged from 1.1 to 49 L/s.

In addition to the volumetric expanders, a pressure ratio is less than five for a single-stage turbine [212]. The tip speed is another crucial

Table 3
Recommendation for selecting expansion machines in CAES systems.

Expansion machine type		Recommended CAES system scale	Recommended operational condition	Recommended CAES system types
Reciprocating machine		Micro-scale CAES and small-scale CAES	High pressure ratio, low rotation speed	I-CAES, and A-CAES
Rotary positive displacement	Scroll	Micro-scale CAES	Medium pressure ratio and low rotation speed	I-CAES, and A-CAES
	Screw	Small-scale CAES	Medium pressure ratio and low rotation speed	I-CAES, and A-CAES
Turbo-machines	Radial turbine	Small-scale and large scale	High rotation speed and low pressure ratio of single-stage	A-CAES
	Axial turbine	Large scale	High rotation speed and low pressure ratio of single-stage	A-CAES, D-CAES

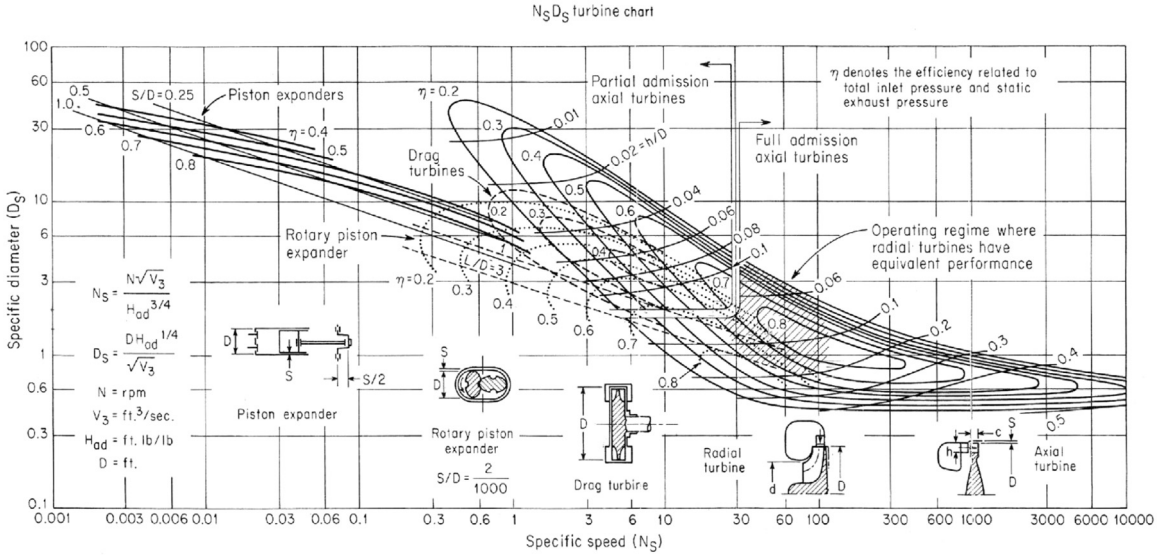

Fig. 12. Performance chart of expansion machines subject to specific speed Ns and specific diameter Ds [209].

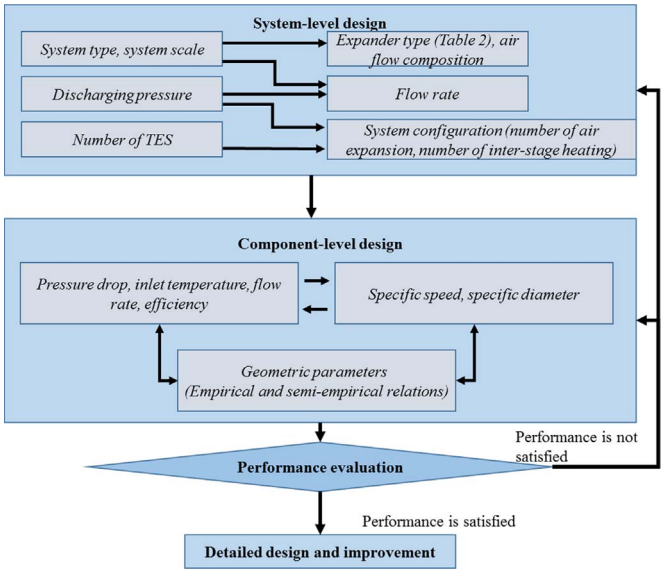

Fig. 13. Flowchart of the preliminary design loop.

factor of determining the centrifugal loading and limiting the operation of a turbine. If the centrifugal stress is excessively large which is beyond the strength of the selected material, the blade would suffer structural failure and fatigue problems. A limiting tip speed of 370 m/s was indicated by Lemort et al. [34]. To avoid the supersonic expansion and the shock loss, the relative Mach number at rotor exit needs to be less than 1. A value of 0.85 was recommended in [34]. The maximum Mach number in the turbine nozzle might be also limited because a high value decreases the efficiency of the turbine. Although most turbine manufactures allow the nozzle flow to be supersonic, Lemort et al. recommended a maximum value of 1.8 [34].

Using the "TICC-500" pilot system as an example [207], the preliminary design loop of the expanders selection is illustrated. 'TICC-500' is a small-scale A-CAES system with sensible heat storage, 500 kW discharging power rating, 2.5 MPa discharging pressure, and up to 120 °C pressurised water as heat storage. To maximise the expansion work of the A-CAES system, the pressure 2.5 MPa is designed for discharging process and then it is reduced to the atmosphere pressure after the expansion, in which three-stage air expansion is selected with an averaged pressure ratio ~ 2.9. The pressure ratios of stages can be estimated analytically by maximising the expansion work with the assumed expander efficiencies and inter-stage heating conditions. Normally, the pressure ratio increases as the compressed air flow is expanded to a large volume flow rate. With the assumed dry air flow, 80% polytropic efficiency of the three expanders and 100 °C inlet air temperature, the average specific enthalpy drop of the expansion-stage is calculated using Eq. (5), which is about 78,619 J/kg. Because the discharging power rating is 500 kW, the averaged mass flow rate is about 2.12 kg/s. And hence, the estimated volumetric flow rates of the three stages are 0.17 m^3/s, 0.45 m^3/s, and 1.66 m^3/s. Due to the small-scale CAES system and large volumetric flow rates through the expanders, the radial turbine is a proper machine type to choose based on Table 3. The high rotational speed of turbines requires extra transmission devices for connection with the generators. With a presumed rotating speed of the turbine, the specific speed can be estimated based on Eq. (7), and the specific diameter is able to find from Fig. 12. Furthermore, using the geometry-based empirical or semi-empirical

models of the radial turbines, with the estimated operating parameters, other preliminary geometric parameters of the radial turbines can be calculated. In practice, prior experiences in the system and components design will accelerate the procedure. Another method is to incorporate optimisation algorithms in the loop for searching the optimum geometric parameters. When the performance of the turbines is satisfied at the preliminary design level, a more detailed design of turbines will continue, such as 2D or 3D impeller design.

5. Conclusions

In the study, an updated review of the CAES applications and the expansion machines in different types are presented. Based on the identified characteristics of both systems and expanders, selection criteria of the matched expansion machines are recommended according to the CAES system type and specifications. Based on the review, some conclusions can be drawn:

1) Three main CAES systems, i.e. D-CAES, A-CAES and I-CAES, are used in energy storage systems, from micro-scale to large-scale. D-CAES is a mature technology which has the lowest cost for the large-scale systems. A-CAES and I-CAES are still at the stage of pre-commercialised. Further studies and projects need to verify the expected performance and analyse the cost-effectiveness of the systems.
2) The volumetric expanders are low cost, low operational speed rotating and easily restructured from available volumetric compressors. The advantages make them ideal choices for micro-scale and small-scale CAES systems.
3) The volumetric expanders are suitable for I-CAES systems because of the tolerance of moisture and two-phase flows in the expansion process.
4) Turbomachines are more appropriate for large-scale D-CAES and A-CAES systems. It is difficult to use turbines in I-CAES systems because of the potential blade erosion.
5) An up-to-date review of empirical models, semi-empirical models and some of the geometry-based models of expanders are presented. The paper reviewed the models with different resolution and accuracy, and discussed the compatibility of these models to be integrated to the system-level modelling and design.
6) This paper proposed a generic procedure of configuring the expansion and inter-stage heating stages, and preliminary designing the selected expanders. It provides an approach for choosing and designing suitable expansion machines to achieve high efficiency of CAES systems.

Coping with the limitations discussed, future developments of expanders for high-performance CAES systems may include:

1) Novel designs of the turbines used in high-pressure and high-temperature D-CAES and A-CAES systems are needed to minimise the pressure drop and increase the power output.
2) Increase of the capacity of volumetric expanders, including reciprocating, screw, and scroll expanders, will increase the applicability of these machines in the small-scale CAES systems and reduce the system economic cost.
3) Pilot systems with volumetric expanders and radial expanders are needed for evaluating the performance of these machines, improving the accuracy of expanders' mathematical models, and gaining experiences for future design.
4) Pilot testing and scaled-up testing of the A-CAES and I-CAES systems are needed for verifying the expected performance and analysing the system cost.
5) Optimal control is another important step to ensure the functionality of the CAES systems and the preferred performance of expanders.

Acknowledgement

Thanks to the funding support from Engineering and Physical Science Research Council (EPSRC), UK (EP/L014211/1 and EP/K002228/1). The authors also want to thank the support from China 973 Research Programme (2015CB251301) to enable the discussion with Chinese partners.

References

[1] Alshehry AS, Belloumi M. Energy consumption, carbon dioxide emissions and economic growth: the case of Saudi Arabia. Renew Sustain Energy Rev 2015;41:237–47.
[2] He W, Wang Y, Shaheed MH. Energy and thermodynamic analysis of power generation using a natural salinity gradient based pressure retarded osmosis process. Desalination 2014;350:86–94.
[3] Weitemeyer S, Kleinhans D, Vogt T, Agert C. Integration of renewable energy sources in future power systems: the role of storage. Renew Energy 2015;75:14–20.
[4] Mathiesen BV, Lund H, Connolly D, Wenzel H, Østergaard PA, Möller B, et al. Smart energy systems for coherent 100% renewable energy and transport solutions. Appl Energy 2015;145:139–54.
[5] Quan H, Srinivasan D, Khambadkone AM, Khosravi A. A computational framework for uncertainty integration in stochastic unit commitment with intermittent renewable energy sources. Appl Energy 2015;152:71–82.
[6] REN21. Renewables 2015: Global Status Report. 2015 [Accessed 18 September 2015]. 〈http://www.ren21.net/wp-content/uploads/2015/07/GSR2015_KeyFindings_lowres.pdf〉.
[7] Arbabzadeh M, Johnson JX, Keoleian GA, Thompson LT, Rasmussen PG. Twelve principles for green energy storage in grid applications. Environ Sci Technol 2015.
[8] Harsha P, Dahleh M. Optimal management and sizing of energy storage under dynamic pricing for the efficient integration of renewable energy. IEEE Trans Power Syst 2015;30:1164–81.
[9] Pérez AA, Vogt T. Life cycle assessment of conversion processes for the large-scale underground storage of electricity from renewables in Europe. In: Proceedings of the EPJ web of conferences: EDP sciences; 2014, p. 03006.
[10] Jiménez Capilla JA, Carrión JA, Alameda-Hernandez E. Optimal site selection for upper reservoirs in pump-back systems, using geographical information systems and multicriteria analysis. Renew Energy 2016;86:429–40.
[11] Zakeri B, Syri S. Electrical energy storage systems: a comparative life cycle cost analysis. Renew Sustain Energy Rev 2015;42:569–96.
[12] The future role for energy storage in the UK main report. Energy Research Partnership (ERP) technology report. 〈http://erpuk.org/wp-content/uploads/2014/10/52990-ERP-Energy-Storage-Report-v3.pdf〉, [Accessed 18 September 2015].
[13] Pimm AJ, Garvey SD, de Jong M. Design and testing of energy bags for underwater compressed air energy storage. Energy 2014;66:496–508.
[14] He W, Luo X, Evans D, Busby J, Garvey S, Parkes D, et al. Exergy storage of compressed air in cavern and cavern volume estimation of the large-scale compressed air energy storage system. Appl Energy.
[15] Mendoza Toledo L, Iglesias A, Favrat D, Schiffmann J. Experimental Investigation of Water Injection in an Oil-Free Co-rotating Scroll Machinery for Compressed Air Energy Storage; 2014.
[16] Minutillo M, Lavadera AL, Jannelli E. Assessment of design and operating parameters for a small compressed air energy storage system integrated with a stand-alone renewable power plant. J Energy Storage 2015.
[17] Li S, Dai Y. Design and simulation analysis of a small-scale compressed air energy storage system directly driven by vertical axis wind turbine for isolated areas. J Energy Eng 2014:04014032.
[18] Farzaneh-Gord M, Izadi S, Pishbin SI, Sheikhani H, Deymi-Dashtebayaz M. Thermodynamic analysis of medium pressure reciprocating natural gas expansion engines. Pol J Chem Technol 2015;17:119–25.
[19] Lu L, Han X, Li J, Hua J, Ouyang M. A review on the key issues for lithium-ion battery management in electric vehicles. J Power Sources 2013;226:272–88.
[20] El-Kady MF, Kaner RB. Scalable fabrication of high-power graphene micro-supercapacitors for flexible and on-chip energy storage. Nat Commun 2013;4:1475.
[21] Luo X, Wang J, Dooner M, Clarke J. Overview of current development in electrical energy storage technologies and the application potential in power system operation. Appl Energy 2015;137:511–36.
[22] Chen H, Cong TN, Yang W, Tan C, Li Y, Ding Y. Progress in electrical energy storage system: a critical review. Prog Nat Sci 2009;19:291–312.
[23] Ibrahim H, Ilinca A, Perron J. Energy storage systems—characteristics and comparisons. Renew Sustain Energy Rev 2008;12:1221–50.
[24] Díaz-González F, Sumper A, Gomis-Bellmunt O, Villafáfila-Robles R. A review of energy storage technologies for wind power applications. Renew Sustain Energy Rev 2012;16:2154–71.
[25] Budt M, Wolf D, Span R, Yan J. A review on compressed air energy storage: basic principles, past milestones and recent developments. Appl Energy 2016;170:250–68.
[26] Marvania D, Subudhi S. A comprehensive review on compressed air powered engine. Renew Sustain Energy Rev 2017;70:1119–30.
[27] Liu J-L, Wang J-H. Thermodynamic analysis of a novel tri-generation system based on compressed air energy storage and pneumatic motor. Energy 2015;91:420–9.
[28] Qiu G, Liu H, Riffat S. Expanders for micro-CHP systems with organic Rankine

cycle. Appl Therm Eng 2011;31:3301–7.
[29] Bao J, Zhao L. A review of working fluid and expander selections for organic Rankine cycle. Renew Sustain Energy Rev 2013;24:325–42.
[30] Lemort V, Quoilin S, Cuevas C, Lebrun J. Testing and modeling a scroll expander integrated into an Organic Rankine Cycle. Appl Therm Eng 2009;29:3094–102.
[31] Quoilin S, Lemort V, Lebrun J. Experimental study and modeling of an Organic Rankine Cycle using scroll expander. Appl Energy 2010;87:1260–8.
[32] Declaye S, Quoilin S, Guillaume L, Lemort V. Experimental study on an open-drive scroll expander integrated into an ORC (Organic Rankine Cycle) system with R245fa as working fluid. Energy 2013;55:173–83.
[33] Lemort V, Declaye S, Quoilin S. Experimental characterization of a hermetic scroll expander for use in a micro-scale Rankine cycle. Proc Inst Mech Eng Part A: J Power Energy 2012;226:126–36.
[34] Lemort V, Guillaume L, Legros A, Declaye S, Quoilin S. A comparison of piston, screw and scroll expanders for small scale Rankine cycle systems. In: Proceedings of the 3rd international conference on microgeneration and related technologies; 2013.
[35] Salvini C, Mariotti P, Giovannelli A. Compression and air storage systems for small size CAES plants: design and off-design analysis. Energy Procedia 2017;107:369–76.
[36] Kim Y, Favrat D. Energy and exergy analysis of a micro-compressed air energy storage and air cycle heating and cooling system. Energy 2010;35:213–20.
[37] Luo X, Wang J, Krupke C, Wang Y, Sheng Y, Li J, et al. Modelling study, efficiency analysis and optimisation of large-scale adiabatic compressed air energy storage systems with low-temperature thermal storage. Appl Energy 2016;162:589–600.
[38] Succar S, Williams RH. Compressed air energy storage: theory, resources, and applications for wind power. New Jersey, USA: Princeton environmental institute report; 2008. p. 8.
[39] Curran H. Use of organic working fluids in Rankine engines. Columbia, MD, USA: Hittman Associates, Inc.; 1979.
[40] Crotogino F, Mohmeyer K, Scharf R, Huntorf C. More than 20 years of successful operation. Orlando, Florida, USA: Meeting of the Solution Mining Research Institute; 2001.
[41] Bagdanavicius A, Jenkins N. Exergy and exergoeconomic analysis of a compressed air energy storage combined with a district energy system. Energy Convers Manag 2014;77:432–40.
[42] Schoenung SM, Eyer JM, Iannucci JJ, Horgan SA. Energy storage for a competitive power market. Annu Rev Energy Environ 1996;21:347–70.
[43] Cheung B, Cao N, Carriveau R, Ting DS-K. Distensible air accumulators as a means of adiabatic underwater compressed air energy storage. Int J Environ Stud 2012;69:566–77.
[44] Grazzini G, Milazzo A. Thermodynamic analysis of CAES/TES systems for renewable energy plants. Renew Energy 2008;33:1998–2006.
[45] Garrison JB, Webber ME. An integrated energy storage scheme for a dispatchable solar and wind powered energy systems. J Renew Sustain Energy 2011;3:043101.
[46] Guo Z, Deng G, Fan Y, Chen G. Performance optimization of adiabatic compressed air energy storage with ejector technology. Appl Therm Eng 2016;94:193–7.
[47] Minutillo M, Lubrano Lavadera A, Jannelli E. Assessment of design and operating parameters for a small compressed air energy storage system integrated with a stand-alone renewable power plant. J Energy Storage.
[48] Power R. ADELE–Adiabatic Compressed-Air Energy Storage For Electricity Supply; 2012.
[49] IET. Institute of Engineering Thermophysics, China Science Academy, Advanced compressed air energy storage won the first prize of Beijing science and technology. ⟨http://www.escn.com.cn/news/show-222217.html⟩, [Accessed Jan 2016].
[50] Yang K, Zhang Y, Li X, Xu J. Theoretical evaluation on the impact of heat exchanger in advanced adiabatic compressed air energy storage system. Energy Convers Manag 2014;86:1031–44.
[51] Hartmann N, Vöhringer O, Kruck C, Eltrop L. Simulation and analysis of different adiabatic compressed air energy storage plant configurations. Appl Energy 2012;93:541–8.
[52] Barbour E, Mignard D, Ding Y, Li Y. Adiabatic compressed air energy storage with packed bed thermal energy storage. Appl Energy 2015;155:804–15.
[53] Wolf D, Budt M. LTA-CAES – a low-temperature approach to adiabatic compressed air energy storage. Appl Energy 2014;125:158–64.
[54] Kim YM, Favrat D. Energy and exergy analysis of a micro-compressed air energy storage and air cycle heating and cooling system. Energy 2010;35:213–20.
[55] Knowlen C, Williams J, Mattick A, Deparis H, Hertzberg A. Quasi-isothermal expansion engines for liquid nitrogen automotive propulsion. SAE Technical Paper; 1997.
[56] Bollinger BR. System and method for rapid isothermal gas expansion and compression for energy storage. Google Patents; 2010.
[57] Bell IH, Lemort V, Groll EA, Braun JE, King GB, Horton WT. Liquid-flooded compression and expansion in scroll machines – Part I: model development. Int J Refrig 2012;35:1878–89.
[58] Bell IH, Lemort V, Groll EA, Braun JE, King GB, Horton WT. Liquid flooded compression and expansion in scroll machines – Part II: experimental testing and model validation. Int J Refrig 2012;35:1890–900.
[59] Lemort V, Bell I, Groll EA, Braun J. Analysis of liquid-flooded expansion using a scroll expander; 2008.
[60] Van de Ven JD, Li PY. Liquid piston gas compression. Appl Energy 2009;86:2183–91.
[61] Qin C, Loth E. Liquid piston compression efficiency with droplet heat transfer. Appl Energy 2014;114:539–50.
[62] Park J-k, Ro PI, He X, Mazzoleni AP. Analysis and Proof-of-Concept Experiment of Liquid-Piston Compression for Ocean Compressed Air Energy Storage (OCAES) System; 2014.
[63] Saadat M, Shirazi FA, Li PY. Modeling and control of an open accumulator compressed air energy storage (CAES) system for wind turbines. Appl Energy 2015;137:603–16.
[64] Yan B, Wieberdink J, Shirazi F, Li PY, Simon TW, Van, et al. Experimental study of heat transfer enhancement in a liquid piston compressor/expander using porous media inserts. Appl Energy 2015;154:40–50.
[65] Sustain X. SustainX's ICAESTM. ⟨http://www.sustainx.com/technology-isothermal-caes.htm⟩, [Accessed June 2016].
[66] LightSail Energy. ⟨http://www.lightsail.com/⟩, [Accessed June 2016].
[67] Shen J, Xing Z, Zhang K, He Z, Wang X. Development of a water-injected twin-screw compressor for mechanical vapor compression desalination systems. Appl Therm Eng 2016;95:125–35.
[68] James NA, Braun JE, Groll EA, Horton WT. Semi-empirical modeling and analysis of oil flooded R410A scroll compressors with liquid injection for use in vapor compression systems. Int J Refrig.
[69] Foley A, Díaz Lobera I. Impacts of compressed air energy storage plant on an electricity market with a large renewable energy portfolio. Energy 2013;57:85–94.
[70] Kere A, Sadiki N, Py X, Goetz V. Applicability of thermal energy storage recycled ceramics to high temperature and compressed air operating conditions. Energy Convers Manag 2014;88:113–9.
[71] Bullough C, Gatzen C, Jakiel C, Koller M, Nowi A, Zunft S. Advanced adiabatic compressed air energy storage for the integration of wind energy. In: Proceedings of the European wind energy conference, EWEC; 2004, p. 25.
[72] Liu J-L, Wang J-H. A comparative research of two adiabatic compressed air energy storage systems. Energy Convers Manag 2016;108:566–78.
[73] Dinter F, Geyer MA, Tamme R. Thermal energy storage for commercial applications: a feasibility study on economic storage systems. Berlin, Germany: Springer; 1991.
[74] Geyer M. Thermal storage for solar power plants. Solar power plants. Springer; 1991. p. 199–214.
[75] Yang Z, Wang Z, Ran P, Li Z, Ni W. Thermodynamic analysis of a hybrid thermal-compressed air energy storage system for the integration of wind power. Appl Therm Eng 2014;66:519–27.
[76] Peng H, Li R, Ling X, Dong H. Modeling on heat storage performance of compressed air in a packed bed system. Appl Energy 2015;160:1–9.
[77] Zavattoni S, Barbato M, Geissbühler L, Haselbacher A, Zanganeh G, Steinfeld A. CFD modeling and experimental validation of a high-temperature pilot-scale combined sensible/latent thermal energy storage; 2015.
[78] Peng H, Dong H, Ling X. Thermal investigation of PCM-based high temperature thermal energy storage in packed bed. Energy Convers Manag 2014;81:420–7.
[79] Oró E, de Gracia A, Castell A, Farid MM, Cabeza LF. Review on phase change materials (PCMs) for cold thermal energy storage applications. Appl Energy 2012;99:513–33.
[80] Kenisarin M, Mahkamov K. Passive thermal control in residential buildings using phase change materials. Renew Sustain Energy Rev 2016;55:371–98.
[81] Zhou Z, Zhang Z, Zuo J, Huang K, Zhang L. Phase change materials for solar thermal energy storage in residential buildings in cold climate. Renew Sustain Energy Rev 2015;48:692–703.
[82] Gil A, Medrano M, Martorell I, Lazaro A, Dolado P, Zalba B, et al. State of the art on high temperature thermal energy storage for power generation. Part 1—concepts, materials and modellization. Renew Sustain Energy Rev 2010;14:31–55.
[83] Hale M. Survey of thermal storage for parabolic trough power plants [No. NREL/SR-550-27925]. Golden, CO, USA: NREL Report; 2000. p. 1–28.
[84] Tian Y, Zhao CY. A review of solar collectors and thermal energy storage in solar thermal applications. Appl Energy 2013;104:538–53.
[85] Tessier MJ, Floros MC, Bouzidi L, Narine SS. Exergy analysis of an adiabatic compressed air energy storage system using a cascade of phase change materials. Energy 2016;106:528–34.
[86] Park J-k, Ro PI, Lim SD, Mazzoleni AP, Quinlan B. Analysis and optimization of a quasi-isothermal compression and expansion cycle for ocean compressed air energy storage (OCAES). Oceans 2012;2012:1–8.
[87] Yan B. Compression/expansion within a cylindrical chamber: application of a liquid piston and various porous inserts. Minneapolis, MN, USA: University of Minnesota; 2013.
[88] Zhang C, Yan B, Wieberdink J, Li PY, Van de Ven JD, Loth E, et al. Thermal analysis of a compressor for application to Compressed Air Energy Storage. Appl Therm Eng 2014;73:1402–11.
[89] Xing Luo JW. Overview of current development of compressed air energy storage; 2013.
[90] Wallace F. Theoretical assessment of the performance characteristics of inward radial flow turbines. Proc Inst Mech Eng 1958;172:931–52.
[91] Nakhamkin M. 15 MW CAES Plant with Above Ground Storage – Distributed Generation based on Novel Concepts Developed by ESPC; 2012.
[92] Liu W, Liu L, Zhou L, Huang J, Zhang Y, Xu G, et al. Analysis and optimization of a compressed air energy storage—combined cycle system. Entropy 2014;16:3103–20.
[93] Zhao P, Gao L, Wang J, Dai Y. Energy efficiency analysis and off-design analysis of two different discharge modes for compressed air energy storage system using axial turbines. Renew Energy 2016;85:1164–77.
[94] Jannelli E, Minutillo M, Lubrano Lavadera A, Falcucci G. A small-scale CAES (compressed air energy storage) system for stand-alone renewable energy power plant for a radio base station: a sizing-design methodology. Energy 2014;78:313–22.
[95] Grazzini G, Milazzo A. A thermodynamic analysis of multistage adiabatic CAES.

Proc IEEE 2012;100:461–72.
[96] Kim Y-M, Lee J-H, Kim S-J, Favrat D. Potential and evolution of compressed air energy storage: energy and exergy analyses. Entropy 2012;14:1501–21.
[97] White AJ, McTigue JD, Markides CN. Analysis and optimisation of packed-bed thermal reservoirs for electricity storage applications. Proc Inst Mech Eng Part A: J Power Energy 2016;230:739–54.
[98] MIT Technology Review. The Energy Startup Conumdrum; 2015.
[99] Najjar YH, Jubeh N. Comparison of performance of compressed-air energy-storage plant with compressed-air storage with humidification. Proc Inst Mech Eng Part A: J Power Energy 2006;220:581–8.
[100] Zhao P, Dai Y, Wang J. Performance assessment and optimization of a combined heat and power system based on compressed air energy storage system and humid air turbine cycle. Energy Convers Manag 2015;103:562–72.
[101] Cheung BC, Carriveau R, Ting DSK. Parameters affecting scalable underwater compressed air energy storage. Appl Energy 2014;134:239–47.
[102] Cheung BC, Carriveau R, Ting DSK. Multi-objective optimization of an underwater compressed air energy storage system using genetic algorithm. Energy 2014;74:396–404.
[103] Slocum AH, Fennell GE, Dundar G, Hodder BG, Meredith JD, Sager MA. Ocean renewable energy storage (ORES) system: analysis of an undersea energy storage concept. Proc IEEE 2013;101:906–24.
[104] Lim SD, Mazzoleni AP, Park J-k, Ro PI, Quinlan B. Conceptual design of ocean compressed air energy storage system. Oceans 2012;2012:1–8.
[105] Pimm A, Garvey S. Analysis of flexible fabric structures for large-scale subsea compressed air energy storage. J Phys: Conf Ser 2009:012049.
[106] Ameel B, T'Joen C, De Kerpel K, De Jaeger P, Huisseune H, Van Belleghem M, et al. Thermodynamic analysis of energy storage with a liquid air Rankine cycle. Appl Therm Eng 2013;52:130–40.
[107] Morgan R, Nelmes S, Gibson E, Brett G. Liquid air energy storage – analysis and first results from a pilot scale demonstration plant. Appl Energy 2015;137:845–53.
[108] Guizzi GL, Manno M, Tolomei LM, Vitali RM. Thermodynamic analysis of a liquid air energy storage system. Energy 2015;93(Part2):1639–47.
[109] Highview Power Storage. 〈http://www.highview-power.com/pre-commercial-laes-technology-demonstrator-online-end-of-2015/〉, [Accessed March 2016].
[110] Guo H, Xu Y, Chen H, Zhou X. Thermodynamic characteristics of a novel supercritical compressed air energy storage system. Energy Convers Manag 2016;115:167–77.
[111] Wang M, Zhao P, Yang Y, Dai Y. Performance analysis of energy storage system based on liquid carbon dioxide with different configurations. Energy 2015;93(Part2):1931–42.
[112] Brown RN. Compressors: selection and sizing. Huston, TX, USA: Gulf Professional Publishing; 1997.
[113] Hyland R, Wexter A. Formulations for the thermodynamic properties of dry air from 173.15 K to 473.15 K, and of saturated moist air from 173.15 K to 372.15 K, at pressures to 5 MPa. ASHRAE Trans 1983;89:520–35.
[114] Goff JA, Gratch S. Thermodynamic properties of moist air. ASHVE Trans 1945;51:125–58.
[115] Ji X, Yan J. Thermodynamic properties for humid gases from 298 to 573 K and up to 200 bar. Appl Therm Eng 2006;26:251–8.
[116] Herrmann S, Kretzschmar H-J, Teske V, Vogel E, Ulbig P, Span R, et al. Properties of humid air for calculating power cycles. J Eng Gas Turbines Power 2010;132:093001.
[117] Herrmann S, Kretzschmar H-J, Gatley DP. Thermodynamic properties of real moist air, dry air, steam, water, and ice (RP-1485). HVAC&R Res 2009;15:961–86.
[118] Lemmon EW, Huber ML, McLinden MO. NIST reference fluid thermodynamic and transport properties–REFPROP. version; 2002.
[119] Bell IH, Wronski J, Quoilin S, Lemort V. Pure and pseudo-pure fluid thermophysical property evaluation and the open-source thermophysical property library CoolProp. Ind Eng Chem Res 2014;53:2498–508.
[120] Damle R, Rigola J, Pérez-Segarra CD, Castro J, Oliva A. Object-oriented simulation of reciprocating compressors: numerical verification and experimental comparison. Int J Refrig 2011;34:1989–98.
[121] Wang X, Zhao L, Wang J, Zhang W, Zhao X, Wu W. Performance evaluation of a low-temperature solar Rankine cycle system utilizing R245fa. Sol Energy 2010;84:353–64.
[122] Hua T, Yitai M, Minxia L, Haiqing G, Zhongyan L. Influence of a non-condensable gas on the performance of a piston expander for use in carbon dioxide trans-critical heat pumps. Appl Therm Eng 2011;31:1943–9.
[123] Demler RL. The application of the positive displacement reciprocating steam expander to the passenger car. SAE Technical Paper; 1976.
[124] Glavatskaya Y, Podevin P, Lemort V, Shonda O, Descombes G. Reciprocating expander for an exhaust heat recovery rankine cycle for a passenger car application. Energies 2012;5:1751–65.
[125] Wronski J, Oudkerk J-F, Haglind F. Modelling of a small scale reciprocating ORC expander for cogeneration applications. In: Proceedings of the ASME ORC 2nd international seminar on ORC power systems; 2013.
[126] Oudkerk J-F, Dickes R, Dumont O, Lemort V. Experimental performance of a piston expander in a small-scale organic Rankine cycle. IOP Conf Ser: Mater Sci Eng 2015:012066.
[127] Wang J, Xu W, Ding S, Shi Y, Cai M, Rehman A. Liquid air fueled open-closed cycle Stirling engine and its exergy analysis. Energy 2015;90(Part1):187–201.
[128] Wang T, Zhang Y, Peng Z, Shu G. A review of researches on thermal exhaust heat recovery with Rankine cycle. Renew Sustain Energy Rev 2011;15:2862–71.
[129] Baek J, Groll E, Lawless P. Piston-cylinder work producing expansion device in a transcritical carbon dioxide cycle. Part I: experimental investigation. Int J Refrig 2005;28:141–51.
[130] Zhang B, Peng X, He Z, Xing Z, Shu P. Development of a double acting free piston expander for power recovery in transcritical CO_2 cycle. Appl Therm Eng 2007;27:1629–36.
[131] Teng H, Regner G, Cowland C. Waste heat recovery of heavy-duty diesel engines by organic Rankine cycle Part I: hybrid energy system of diesel and Rankine engines. SAE Technical Paper; 2007.
[132] Teng H, Regner G, Cowland C. Achieving high engine efficiency for heavy-duty diesel engines by waste heat recovery using supercritical organic-fluid Rankine cycle. SAE Technical Paper; 2006.
[133] Farzaneh-Gord M, Jannatabadi M. Timing optimization of single-stage single-acting reciprocating expansion engine based on exergy analysis. Energy Convers Manag 2015;105:518–29.
[134] Saadat M, Li PY. Combined optimal design and control of a near isothermal liquid piston air compressor/expander for a compressed air energy storage (CAES) system for wind turbines.
[135] Shepard TG, Lee J, Yan B, Strykowski PJ. Parameters affecting bubble formation and size distribution from porous media. J Fluids Eng 2016;138:031202.
[136] Winandy E, Saavedra OC, Lebrun J. Simplified modelling of an open-type reciprocating compressor. Int J Therm Sci 2002;41:183–92.
[137] Duprez M-E, Dumont E, Frère M. Modelling of reciprocating and scroll compressors. Int J Refrig 2007;30:873–86.
[138] Navarro E, Granryd E, Urchueguía JF, Corberán JM. A phenomenological model for analyzing reciprocating compressors. Int J Refrig 2007;30:1254–65.
[139] Mathie R, Markides CN, White AJ. A framework for the analysis of thermal losses in reciprocating compressors and expanders. Heat Transf Eng 2014;35:1435–49.
[140] McKay RA. International test and demonstration of a 1-MW wellhead generator: Helical screw expander power plant; 1984.
[141] Wang W, Wu Y-t, Xia G-d, Ma C-f, Wang J-f, Zhang Y. Experimental study on the performance of the single screw expander prototype by optimizing configuration. In: Proceedings of the ASME 2012 6th international conference on energy sustainability collocated with the ASME 2012 10th international conference on fuel cell science, engineering and technology, American Society of Mechanical Engineers; 2012, p. 1281–6.
[142] Taniguchi H, Kudo K, Giedt W, Park I, Kumazawa S. Analytical and experimental investigation of two-phase flow screw expanders for power generation. J Eng Gas Turbines Power 1988;110:628–35.
[143] Xia G-D, Zhang Y-Q, Wu Y-T, Ma C-F, Ji W-N, Liu S-W, et al. Experimental study on the performance of single-screw expander with different inlet vapor dryness. Appl Therm Eng 2015;87:34–40.
[144] Kaneko T, Hirayama N. Study on fundamental performance of helical screw expander. Bull JSME 1985;28:1970–7.
[145] Imran M, Usman M, Park B-S, Lee D-H. Volumetric expanders for low grade heat and waste heat recovery applications. Renew Sustain Energy Rev 2016;57:1090–109.
[146] Li J, Feng Q, Liu F, Wu W. Experimental studies of the tooth wear resistance with different profiles in single screw compressor. Tribol Int 2013;57:210–5.
[147] Clemente S, Micheli D, Reini M, Taccani R. Energy efficiency analysis of Organic Rankine Cycles with scroll expanders for cogenerative applications. Appl Energy 2012;97:792–801.
[148] Kim H, Ahn J, Park I, Rha P. Scroll expander for power generation from a low-grade steam source. Proc Inst Mech Eng Part A: J Power Energy 2007;221:705–11.
[149] He W, Wu Y, Peng Y, Zhang Y, Ma C, Ma G. Influence of intake pressure on the performance of single screw expander working with compressed air. Appl Therm Eng 2013;51:662–9.
[150] Ziviani D, Bell IH, De Paepe M, van den Broek M. Update on single-screw expander geometry model integrated into an open-source simulation tool. IOP Conf Ser: Mater Sci Eng 2015:012064.
[151] Desideri A, Van Den Broek M, Gusev S, Lemort V, Quoilin S. Experimental campaign and modeling of a low-capacity waste heat recovery system based on a single screw expander; 2014.
[152] Stosic N, Smith IK, Kovacevic A. A twin screw combined compressor and expander for CO_2 refrigeration systems; 2002.
[153] Tang H, Wu H, Wang X, Xing Z. Performance study of a twin-screw expander used in a geothermal organic Rankine cycle power generator. Energy 2015;90(Part1):631–42.
[154] Peris B, Navarro-Esbrí J, Molés F, Collado R, Mota-Babiloni A. Performance evaluation of an Organic Rankine Cycle (ORC) for power applications from low grade heat sources. Appl Therm Eng 2015;75:763–9.
[155] Krupke C, Wang J, Clarke J, Luo X. Dynamic modelling of a hybrid wind turbine in connection with compressed air energy storage through a power split transmission device. In: Proceedings of the advanced intelligent mechatronics (AIM), 2015 IEEE international conference on: IEEE; 2015, p. 79–84.
[156] Sun H, Luo X, Wang J. Feasibility study of a hybrid wind turbine system – integration with compressed air energy storage. Appl Energy 2015;137:617–28.
[157] Igobo ON, Davies PA. Review of low-temperature vapour power cycle engines with quasi-isothermal expansion. Energy 2014;70:22–34.
[158] Iglesias A, Favrat D. Innovative isothermal oil-free co-rotating scroll compressor–expander for energy storage with first expander tests. Energy Convers Manag 2014;85:565–72.
[159] Comfort III W. Design and evaluation of a two-phase turbine for low quality steam–water mixtures. Livermore, USA: Lawrence Livermore Lab., California Univ.; 1977.
[160] Margolis DL. Analytical modeling of helical screw turbines for performance prediction. J Eng Power 1978;100:482–7.
[161] Avadhanula VK, Lin C-S. Empirical models for a screw expander based on experimental data from organic Rankine cycle system testing. J Eng Gas Turbines

Power 2014;136:062601.
[162] Ziviani D, van den Broek M, De Paepe M. Geometry-based modeling of single screw expander for Organic Rankine Cycle systems in low-grade heat recovery. Energy Procedia 2014;61:100–3.
[163] Ziviani D, Bell I, van den Broek M, De Paepe M. Comprehensive Model of a Single-screw Expander for ORC-Systems; 2014.
[164] Winandy E, Saavedra C, Lebrun J. Experimental analysis and simplified modelling of a hermetic scroll refrigeration compressor. Appl Therm Eng 2002;22:107–20.
[165] Quoilin S, Declaye S, Legros A, Guillaume L, Lemort V. Working fluid selection and operating maps for Organic Rankine Cycle expansion machines. In: Proceedings of the 21st international compressor conference at Purdue; 2012, p. 10.
[166] Quoilin S, Aumann R, Grill A, Schuster A, Lemort V, Spliethoff H. Dynamic modeling and optimal control strategy of waste heat recovery Organic Rankine Cycles. Appl Energy 2011;88:2183–90.
[167] Twomey B, Jacobs PA, Gurgenci H. Dynamic performance estimation of small-scale solar cogeneration with an organic Rankine cycle using a scroll expander. Appl Therm Eng 2013;51:1307–16.
[168] Guangbin L, Yuanyang Z, Liansheng L, Pengcheng S. Simulation and experiment research on wide ranging working process of scroll expander driven by compressed air. Appl Therm Eng 2010;30:2073–9.
[169] Guangbin L, Yuanyang Z, Yunxia L, Liansheng L. Simulation of the dynamic processes in a scroll expander—generator used for small-scale organic Rankine cycle system. Proc Inst Mech Eng Part A: J Power Energy 2011;225:141–9.
[170] Wang J, Yang L, Luo X, Mangan S, Derby JW. Mathematical modeling study of scroll air motors and energy efficiency analysis—Part I. IEEE/ASME Trans Mechatron 2011;16:112–21.
[171] Wang J, Luo X, Yang L, Shpanin LM, Jia N, Mangan S, et al. Mathematical modeling study of scroll air motors and energy efficiency analysis—Part II. IEEE/ASME Trans Mechatron 2011;16:122–32.
[172] Paltrinieri A. A mean-line model to predict the design performance of radial inflow turbines in organic rankine cycles; 2014.
[173] Baskharone EA. Principles of turbomachinery in air-breathing engines. Cambridge, UK: Cambridge University Press; 2006.
[174] Sauret E, Rowlands AS. Candidate radial-inflow turbines and high-density working fluids for geothermal power systems. Energy 2011;36:4460–7.
[175] Fiaschi D, Manfrida G, Maraschiello F. Thermo-fluid dynamics preliminary design of turbo-expanders for ORC cycles. Appl Energy 2012;97:601–8.
[176] Kang SH. Design and experimental study of ORC (Organic Rankine Cycle) and radial turbine using R245fa working fluid. Energy 2012;41:514–24.
[177] Watson N, Janota MS. Turbocharging: the internal combustion engine. Basingstoke, United Kingdom: MacMillan; 1982.
[178] Winterbone D. The theory of wave action approaches applied to reciprocating engines. Dordrecht, Netherland: Internal Combustion Engineering: Science & Technology, Springer; 1990. p. 445–500.
[179] Payri F, Desantes J, Boada F. Prediction method for the operating conditions of a turbocharged diesel engine. In: Proceedings of the motor Sympo'86, Praga London; 1986, p. 8–16.
[180] Payri F, Benajes J, Jullien J, Duan Q. Non-steady flow behaviour of a supercharger turbine. In: Proceedings of the third EAEC international conference. Strasbourg; 1991, p. 347–51.
[181] Payri F, Benajes J, Reyes M. Modelling of supercharger turbines in internal-combustion engines. Int J Mech Sci 1996;38:853–69.
[182] Baines N, Hajilouy-Benisi A, Yeo J. The pulse flow performance and modelling of radial inflow turbines. Inst Mech Eng Conf Publ 1994:209. [-].
[183] Serrano JR, Arnau FJ, Dolz V, Tiseira A, Cervelló C. A model of turbocharger radial turbines appropriate to be used in zero- and one-dimensional gas dynamics codes for internal combustion engines modelling. Energy Convers Manag 2008;49:3729–45.
[184] Pesiridis A, Salim W, Martinez-Botas R. Turbocharger matching methodology for improved exhaust energy recovery. In: Proceedings of the 10th international conference on turbochargers and turbocharging. Elsevier; 2012, p. 203–17.
[185] Eriksson L. Modeling and control of turbocharged SI and DI engines. Oil Gas Sci Technol-Rev l'IFP 2007;62:523–38.
[186] Canova M. Development and validation of a control-oriented library for the simulation of automotive engines. Int J Engine Res 2004;5:219–28.
[187] Chen L, Wei M, Yang H. Experiment and simulation of the mean value model on two-stroke gasoline aero-engine. J Aerosp Power 2008;23:2249–55.
[188] Moraal P, Kolmanovsky I. Turbocharger modeling for automotive control applications. SAE Technical Paper; 1999.
[189] Orkisz M, Stawarz S. Modeling of turbine engine axial-flow compressor and turbine characteristics. J Propuls Power 2000;16:336–9.
[190] Fang X, Dai Q. Modeling of turbine mass flow rate performances using the Taylor expansion. Appl Therm Eng 2010;30:1824–31.
[191] Fang X, Chen W, Zhou Z, Xu Y. Empirical models for efficiency and mass flow rate of centrifugal compressors. Int J Refrig 2014;41:190–9.
[192] Wu C-H. A general theory of three-dimensional flow in subsonic and supersonic turbomachines of axial-, radial, and mixed-flow types. DTIC Doc 1952.
[193] Bohn D, Kim T. A comparative throughflow analysis of axial flow turbines. Proc Inst Mech Eng Part A: J Power Energy 1998;212:141–5.
[194] Rahbar K, Mahmoud S, Al-Dadah RK. Mean-line modeling and CFD analysis of a miniature radial turbine for distributed power generation systems. Int J Low-Carbon Technol 2014. [ctu028].
[195] Hu D, Zheng Y, Wu Y, Li S, Dai Y. Off-design performance comparison of an organic Rankine cycle under different control strategies. Appl Energy 2015;156:268–79.
[196] Hu D, Li S, Zheng Y, Wang J, Dai Y. Preliminary design and off-design performance analysis of an Organic Rankine Cycle for geothermal sources. Energy Convers Manag 2015;96:175–87.
[197] Oh HW, Yoon ES, Chung M. An optimum set of loss models for performance prediction of centrifugal compressors. Proc Inst Mech Eng Part A: J Power Energy 1997;211:331–8.
[198] Persson J. 1D Turbine Design Tool Validation and Loss Model Comparison: Performance Prediction of a 1-stage Turbine at Different Pressure Ratios; 2015.
[199] Kacker S, Okapuu U. A mean line prediction method for axial flow turbine efficiency. J Eng Power 1982;104:111–9.
[200] Da Lio L, Manente G, Lazzaretto A. New efficiency charts for the optimum design of axial flow turbines for Organic Rankine Cycles. Energy 2014;77:447–59.
[201] Da Lio L, Manente G, Lazzaretto A. Predicting the optimum design of single stage axial expanders in ORC systems: is there a single efficiency map for different working fluids? Appl Energy 2016;167:44–58.
[202] Axial Turbine Stage, Wikipedia. 〈https://en.wikipedia.org/wiki/Axial_Turbine_Stages〉, [Accessed March 2016].
[203] Mohammadi A, Mehrpooya M. Exergy analysis and optimization of an integrated micro gas turbine, compressed air energy storage and solar dish collector process. J Clean Prod 2016;139:372–83.
[204] Dixon SL, Hall C. Fluid mechanics and thermodynamics of turbomachinery: Butterworth-Heinemann; 2013.
[205] STEPS TO COMPRESSOR SELECTION & SIZING. 〈https://engage.aiche.org/HigherLogic/System/DownloadDocumentFile.ashx?DocumentFileKey=39c1c4a6-7f87-45ca-a5d4-0408fe927f8c&ssopc=1〉, [Accessed 4 July 2017].
[206] Wilson DG, Korakianitis T. The design of high-efficiency turbomachinery and gas turbines. Cambridge, MA, USA: MIT press; 2014.
[207] Wang S, Zhang X, Yang L, Zhou Y, Wang J. Experimental study of compressed air energy storage system with thermal energy storage. Energy 2016;103:182–91.
[208] Sciacovelli A, Li Y, Chen H, Wu Y, Wang J, Garvey S, et al. Dynamic simulation of adiabatic compressed air energy storage (A-CAES) plant with integrated thermal storage – link between components performance and plant performance. Appl Energy 2017;185(Part1):16–28.
[209] Balje O. A study on design criteria and matching of turbomachines: Part A—similarity relations and design criteria of turbines. J Eng Gas Turbines Power 1962;84:83–102.
[210] Latz G, Andersson S, Munch K. Selecting an expansion machine for vehicle waste-heat recovery systems based on the Rankine cycle. SAE Technical Paper; 2013.
[211] Quoilin S, Declaye S, Lemort V. Expansion machine and fluid selection for the organic Rankine cycle. In: Proceedings of the 7th international conference on heat transfer, fluid mechanics and thermodynamics; 2010.
[212] Wong CS. Design-to-Resource (DTR) using SMC Turbine Adaptive Strategy: Design Process of Low Temperature Organic Rankine Cycle (LT-ORC); 2015.